ISTANBUL TECHNICAL UNIVERSITY ★ GRADUATE SCHOOL OF SCIENCE ENGINEERING AND TECHNOLOGY

MODELLING AND STATE OF CHARGE ESTIMATION FOR LITHIUM-ION BATTERIES

M.Sc. THESIS

Ozan ÖZAY

Department of Mechatronics Engineering

Mechatronics Engineering Programme

JUNE 2019

ISTANBUL TECHNICAL UNIVERSITY ★ GRADUATE SCHOOL OF SCIENCE
ENGINEERING AND TECHNOLOGY

MODELLING AND STATE OF CHARGE ESTIMATION FOR LITHIUM-ION BATTERIES

M.Sc. THESIS

Ozan ÖZAY
(518161020)

Department of Mechatronics Engineering

Mechatronics Engineering Programme

Thesis Advisor: Prof. Dr. O. Seta BOĞOSYAN

JUNE 2019

İSTANBUL TEKNİK ÜNİVERSİTESİ ★ FEN BİLİMLERİ ENSTİTÜSÜ

LiTYUM-İYON BATARYALARDA MODELLEME VE ŞARJ DURUMU KESTİRİMİ

YÜKSEK LİSANS TEZİ

Ozan ÖZAY
(518161020)

Mekatronik Mühendisliği Anabilim Dalı

Mekatronik Mühendisliği Programı

Tez Danışmanı: Prof. Dr. O. Seta BOĞOSYAN

HAZİRAN 2019

Ozan ÖZAY, a M.Sc. student of ITU Graduate School of Science Engineering and Technology 518161020 successfully defended the thesis entitled "MODELLING AND STATE OF CHARGE ESTIMATION FOR LITHIUM-ION BATTERIES", which he/she prepared after fulfilling the requirements specified in the associated legislations, before the jury whose signatures are below.

Thesis Advisor :	**Prof. Dr. O. Seta BOĞOSYAN** Istanbul Technical University	....
Jury Members :	**Prof. Dr. Metin GÖKAŞAN** Istanbul Technical University	....
	Asst. Prof. Dr. Taner ARSAN Kadir Has University	....

Date of Submission : **3 May 2019**
Date of Defense : **21 June 2019**

To my love,

FOREWORD

Firstly, I would like to thank my advisor Prof. Dr. O. Seta BOĞOSYAN for her guidance and support. I would like to express my gratitude to Prof. Dr. Metin GÖKAŞAN for the comments and suggestions on this work. Also, I want to thank Dr. Murat DEMİRCİ from FEV Turkey for his orientation and trust in the project.

Finally, I want to thank family for their unconditional support and love.

June 2019 Ozan ÖZAY

TABLE OF CONTENTS

Page

ABBREVIATIONS

Ah	: Ampere-Hour : 1 Ah =3600 Coulomb
BMS	: Battery Management System
BOL	: Beginning of Life
CCCV	: Constant Current Constant Voltage
DOD	: Depth of Discharge(Ah)
E	: Reversible Cell Voltage(V)
ECM	: Equivalent Circuit Model
EOL	: End of Life
EV	: Electric Vehicle
HPPC	: Hybrid Pulse Power Characterization
HV	: High Voltage
I	: Electric Current(A)
Li-ion	:Lithium ion
MOSFET	: Metal oxide semiconductor—field effect transistor
NEDC	: New European Driving Cycle
NMC	: Nickel Manganese Cobalt Oxide
OCV	: Open circuit voltage
P	: Electric Power(W)
Regen	: Regenerative braking
RESS	: Rechargeable Energy Storage System
RUL	: Remaining Useful Life
SOC	: State of Charge(perc)
SOH	: State of Health(perc)
T	: Absolute Temperature(K)
U	: Electric Potential Difference from a Reference(V)
Wh	: Electrical Energy (J = Ws)
Wh kg^{-1}	: Specific Energy(Watt-hours per kilogram)
Wh L^{-1}	: Energy density
W kg^{-1}	: Specific Power(Watts per kilogram)
W L^{-1}	: Power density
WLTP	: Worldwide Harmonized Light Vehicle Test Procedure
xEV	: General name of: Hybrid,Battery,Plug-in and Fuel Cell Electric Vehicles

SYMBOLS

A_k,B_k,C_k,D_k	: State Transition Matrices at The Time Index k
C	: Capacitance
I	: Current
k	: Discrete time index
K	: Kalman Gain Matrix
R	: Resistance
t	: Time
T	: Temperature
Q	: Capacity
u	: Input
x	: State Vector
V	: Voltage
Δ t	: Discrete Time Step

LIST OF TABLES

LIST OF FIGURES

Page

MODELLING AND STATE OF CHARGE ESTIMATION FOR LITHIUM-ION BATTERIES

SUMMARY

Factors such as the decrease in petroleum fuel reserves, the increase in fuel costs and the harmful gases released by the vehicles using petroleum-derived fuels created the need for alternative methods in road transportation.

Over the past two decades, electric vehicles have become a part of road transportation in different forms. Electric vehicles do not need a drivetrain and a gearbox like the vehicles that use petroleum fuel and they can re-use the braking energy with the reclaimed brake method. This situation proves that public transportation could be much more efficient by using electric vehicles. The adoption of hybrid and electric vehicles has accelerated due to the fact that the service needs for electric vehicles are much less than those using petroleum fuels, they have significantly reduced the cost of transportation per kilometer and they have also reduced the release of harmful gases. By reducing the cost of research development towards engine calibration, drivetrain, and gearboxes, electric vehicles have enabled vehicle manufacturers to invest in higher technologies, such as advanced driver assistance systems.

In addition to all these positive developments, some developed countries took various measures to promote the use of electric vehicles. In 2016, the Government Fleet Declaration, signed by the United States, China, Britain, France, Japan, Canada, Norway, and Sweden, announced that these countries would considerably lower their carbon emission rates in the coming years and implement significant investments and sanctions. In Norway, no tax is applied in the purchase of electric vehicles, electric vehicles with very low annual taxes can also be used free of charge, and even ferries that combine international routes are free. If companies rent an electric car, the rental costs are deducted from taxes. Such sanctions set an example for the whole world, revealing the role of governments in this process.

Developed battery technologies combined with newly produced batteries have been in compliance with the automotive standards, while energy costs for energy storage decreased and the amount of energy that could be stored in the same volume and weight increased. Longer-lasting, more reliable batteries have been launched. High power density batteries provide the same acceleration performance as the smaller battery packs for hybrid electric vehicles, while high energy density batteries allow a significant increase in the range of electric vehicles, making electric vehicles preferable for intercity transportation.

With the increase of electric vehicles, the importance of battery packs and battery management systems increased. Batteries with lithium-ion chemistry has gained widespread use in battery packs due to their high energy and power densities, longevity, low self-discharge rate features. The electric vehicle battery pack is composed of many lithium-ion battery cells with 3-4 volts. The voltage increases

when the cells are connected in series and the capacity enhances when the cells are connected in parallel . In high power applications, high voltage battery packs are used to deliver high power with low current. The way to achieve this is to connect several cells in series, the connected cells are charged and discharged with the same current. The cells from the same production line have very similar characteristics, but very small resistance and capacity differences are inevitable. In addition, the different positions of the cells in the package make it difficult for all cells to be at the same temperature at the same time. These situations lead to the formation of charge imbalances between the cells connected in series. When one of the cells connected in series is discharged, the battery pack cannot be used to draw power. Similarly, when one of the cells connected in series is fully charged, the battery pack cannot be charged more, so the charge imbalances prevent the full performance of the battery.
Battery management systems are used to eliminate cell voltage imbalances, to monitor the charging and health status of each cell, to increase the efficiency and life of the cells, to ensure that the cells are operating in proper operating conditions. A battery pack contains many variables that can and cannot be measured. While values such as temperature, current and voltage can be obtained by direct measurement methods, values such as charge status, health status, power condition cannot be measured by direct measurement methods. It is only possible to measure such values by forwarding estimation methods.
The aim of this thesis is to model the battery pack of a hybrid electric vehicle prepared to go to mass production in simulation environment, to estimate the state of charge with the help of Extended Kalman Filter and then to make the battery balancing process according to SOC estimations of Kalman Filter using a battery pack model consisting of 16 cells.
The data required to obtain the model of 51 Ah Lithium-Ion NMC prismatic cells used in the battery pack were obtained from the battery manufacturer. The obtained data were analyzed in detail in MATLAB and used to obtain the cell model and to confirm the obtained model. Ampere-hour counting method which is a simple method which can be applied in the cell simulation model is used, because noise can be prevented in the simulation environment. Ampere-hour counting method which gives very successful results in completely noiseless environment deviates from the real value over time when fed by noisy measurements and it is not possible to correct the deviations by this method (or the cells must have a long-standing state of rest). After the desired convergence is achieved in the cell simulation model, the Extended Kalman filter is designed for charge status estimation. The measurements with noise were used as the inputs of the Kalman filter and the SOC estimates of the Kalman Filter were compared with the SOC estimates of the battery model. This way, the disturbance rejection performance of the designed EKF has been tested.
In addition, situations where the initial charge status is not known, which is very likely to be encountered in real life, have also been tested. For this, the SOC model was given to the battery, while the Kalman filter was initiated with the wrong value and after a short time it was observed that it converged to the correct value successfully.
A battery pack model consisting of 16 cells was created with the cell model generated after the charge condition estimation was successfully designed. A balancing mechanism, that can apply the balancing current to each cell in the package model separately, has been added. The SOC values from the Kalman filter were used to control the balancing mechanism. In terms of simplicity of application, passive balancing method has been preferred. The basic principle of this method is to detect

the cell with the least charge from the series connected cells and to bring all the remaining cell SOC's closer to this value. As a result of the simulation, it is seen that Kalman filter makes accurate predictions despite the package-based noise and is suitable for balancing in real battery packages.

LiTYUM-İYON BATARYALARDA
MODELLEME VE ŞARJ DURUMU KESTİRİMİ

ÖZET

Petrol yakıt rezervlerinin azalması, yakıt maliyetlerinin artması, petrol türevli yakıt kullanan araçların doğaya saldığı zararlı gazlar gibi etkenler karayolu ulaşımında alternatif yöntemlere başvurmayı zorunlu kıldı. Son yirmi yıldır ciddi bir şekilde araştırılan bir konu olan elektrikli araçlar değişik formlarda karayolu ulaşımının bir parçası haline gelmeye başladı. Petrol yakıt kullanan araçlardaki aktarma organlarına ve vites kutusuna ihtiyaç duymayan, frenleme enerjisini geri kazanımlı fren yöntemi ile tekrar kullanabilen elektrikli araçlar, karayolu ulaşımının çok daha verimli bir şekilde yapılabileceğini kamuoyuna gösterdi. Servis ihtiyaçlarının petrol yakıt kullanan araçlara kıyasla çok daha az olması, kilometre başına ulaşım maliyetini ciddi bir şekilde düşürmeleri, zararlı gaz salınımını çok azaltmaları ya da tamamen bitirmeleri toplumun hibrid ve elektrikli araçları kabullenmesini hızlandırdı. Araç üreticilerinin motor kalibrasyonuna, aktarma organlarına ve vites kutularına harcadıkları araştırma geliştirme maliyetlerini kısarak, ileri sürücü yardım sistemleri gibi daha yüksek teknolojilere yatırım yapmasına olanak sağladı.

Bütün bu olumlu gelişmelerin yanı sıra, gelişmiş ülkeler elektrikli araç kullanımını yaygınlaştırmak için çeşitli önlemler aldı, çeşitli imtiyazlar verdi. 2016 yılında ABD, Çin, İngiltere, Fransa, Japonya, Kanada, Norveç ve İsveç arasında imzalanan Hükümet Filo Deklarasyonu(Government Fleet Declaration) ile bu ülkeler gelecek yıllardaki karbon salınım oranlarını ciddi oranda düşüreceklerini ve bu amaç uğruna önemli yatırım ve yaptırımlar uygulayacaklarını ilan ettiler. Ulaşımda elektrikli araç kullanımının en yaygın olduğu ülke olan Norveç'in elektrikli araç sahiplerine verdiği avantajları sıralayacak olursak, elektrikli araç satın alma sürecinde hiçbir vergi uygulanmıyor, yıllık vergileri çok düşük olan elektrikli araçlar ayrıca paralı otoyolları da ücretsiz kullanabiliyor, hatta uluslararası yolları birleştiren feribotları bile ücretsiz kullanabiliyor. Şirketler eğer elektrikli araç kiralarsa, kiralama masrafları vergilerinden düşülüyor. Bu gibi yaptırımlar tüm dünyaya örnek teşkil ederek, hükümetlerin bu süreçte ne kadar önemli bir rolü olabileceğini gözler önüne seriyor.

Gelişen pil teknolojileriyle beraber yeni üretilen piller otomotiv standartlarına uygun bir hale geldi, enerji depolama için maliyetler azalırken, aynı hacim ve ağırlıkta depo edilebilen enerji miktarı arttı. Daha uzun ömürlü, daha güvenilir piller piyasaya sürüldü. Yüksek güç yoğunluklu piller hibrid elektrikli araçlar için daha küçük batarya paketleriyle aynı ivmelenme performansını yakalamaya olanak verirken, yüksek enerji yoğunluklu piller tamamıyla elektrikli araçların menzillerinde ciddi bir artışa imkân vererek elektrikli araçları şehirlerarası ulaşım için de tercih edilebilir kıldı.

Elektrikli araçların artmasıyla birlikte batarya paketlerinin ve batarya yönetim sistemlerinin önemi arttı. Lityum-iyon kimyasına sahip piller, yüksek enerji ve güç yoğunlukları, uzun ömürleri, düşük kendinden boşalma oranları(self discharge rate) gibi özellikleriyle diğer pil kimyalarına üstünlük sağladıkları için batarya paketlerinde yaygın olarak kullanılmaya başlandı. Elektrikli araç batarya paketi 3-4 Voltluk pek çok lityum-iyon batarya hücresinin birleştirilmesinden oluşur. Birbirine paralel bağlanan hücreleri kapasitesi artarken, seri bağlanan hücrelerin gerilimi artar. Elektrikli araçlar gibi yüksek güç gerektiren uygulamalarda, düşük akımla yüksek güç iletebilmek için yüksek gerilimli batarya paketleri kullanılır. Bunu sağlamanın yolu pek çok hücreyi seri olarak bağlamaktan geçer, seri olarak bağlanmış hücreler aynı akımla şarj ve deşarj edilir. Aynı üretim hattından çıkan hücreler çok benzer karakteristik özellikler gösterir, ancak aralarında çok küçük direnç ve kapasite farkları bulunması kaçınılmazdır. Bunların yani sıra hücrelerin paket içindeki konumlarının farklı olması tüm hücrelerin aynı anda aynı sıcaklıkta olmasını zorlaştırır. Bu durumlar seri bağlı hücreler arasında zamanla şarj dengesizliklerinin oluşmasına sebebiyet verir. Batarya paketinde seri bağlı hücrelerin birinin şarjı bittiğinde batarya paketinden güç çekilemez, aynı mantıkla seri bağlı hücrelerin biri tamamen şarj olduğunda batarya paketi daha fazla şarj edilemez, dolayısıyla şarj dengesizlikleri batarya performansının tam olarak kullanılmasına engel olur .

Hücre gerilim dengesizliklerini gidermek, her bir hücrenin şarj ve sağlık durumunu takip etmek, hücrelerin verimini ve ömrünü arttırmak, hücrelerin uygun çalışma koşullarında çalıştığından emin olmak için batarya yönetim sistemleri kullanılır. Bir batarya paketinde ölçülebilir ve ölçülemez pek çok değişken bulunur. Sıcaklık, akım ve voltaj gibi değerler direk ölçüm metotlarıyla elde edilebilirken, şarj durumu, sağlık durumu, güç durumu gibi değerler direk ölçüm metotları ile ölçülemez. Bu gibi değerleri ölçmek ancak ileri kestirim yöntemleriyle mümkündür.

Bu tezin amacı seri üretime gitmek üzere hazırlanan bir hibrid elektrikli aracın batarya paketini simülasyon ortamında modellemek, Şarj durumunu Genişletilmiş Kalman Filtresi yardımıyla kestirebilmek ve sonrasında 16 hücreden oluşan bir batarya paketi modeli kullanarak hücreler arası şarj dengeleme işlemini kalman filtresinin şarj durumu tahminlerine göre yapmaktır. Tez çalışması kapsamında yapılan çalışmalar aşağıdaki paragraflarda sırasıyla açıklanacaktır.

Batarya paketinde kullanılan 51 Ah Lityum-İyon NMC prizmatik hücrelerin modelini elde etmek için gerekli veriler batarya üreticisinden elde edilmiştir. Elde edilen veriler detaylı bir şekilde analiz edilip MATLAB ortamında hücre modeli elde etmekte ve elde edilen modelin doğrulanmasında kullanılmıştır. Hücre simülasyon modelinde uygulanabilirliği basit bir yöntem olan Amper-saat sayma yöntemi kullanılmıştır, çünkü simülasyon ortamında gürültüler engellenebilir. Tamamen gürültüsüz ortamda çok başarılı sonuçlar veren Amper-saat sayma yöntemi, gürültülü ölçümler ile beslendiğinde zamanla gerçek değerden sapar ve bu yöntemle sapmaları düzeltmek ya mümkün değildir ya da hücrelerin uzun süredir dinlenme durumunda olması gerekir. Hücre simülasyon modelinde istenen yakınsama sağlandıktan sonra, şarj durumu kestirimi için Genişletilmiş Kalman filtresi tasarlanmıştır. Batarya modelindeki tamamen gürültüsüz değerler verilirken Kalman filtresinin girişlerine ölçümler gürültülü bir şekilde verilip Kalman Filtresinin şarj durumu tahminleri batarya modelinin şarj durumu tahminleri ile karşılaştırılmıştır. Bu şekilde Tasarlanan EKF'nin bozucu bastırma performansı test edilmiştir. Bunun yanı sıra gerçek hayatta karşımıza çıkması çok muhtemel bir durum olan başlangıç şarj durumunun doğru bilinmediği durumlar da test edilmiştir. Bunun için batarya modeline doğru şarj durumundan başlatılırken, Kalman filtresi yanlış değerden başlatılmış olup kısa bir süre sonra doğru değere başarılı bir şekilde yakınsadığı gözlenmiştir.

Şarj durumu kestirimi işlemi başarılı bir şekilde tasarlandıktan sonra oluşturulan hücre modeli ile 16 hücreden oluşan bir batarya paketi modeli oluşturulmuştur. Paket modelindeki her hücreye ayrı ayrı dengeleme akımı uygulayabilecek, bir balans mekanizması eklenmiştir. Balans mekanizmasının kontrolü için kalman filtresinden çıkan şarj durumu değerleri kullanılmıştır. Uygulama basitliği açısından pasif balans yöntemi tercih edilmiştir, bu yöntemin temel prensibi seri bağlı hücrelerden en az şarjı olan hücreyi tespit edip geri kalan bütün hücre şarj durumlarını bu değere yaklaştırmaktır. Simülasyon sonucunda Kalman filtresinin paket bazında gürültülere rağma doğru tahminler yaptığı ve gerçek batarya paketlerinde dengeleme işlemleri için uygun olduğu görülmüştür.

1. INTRODUCTION

Lithium-ion (Li-ion) cells become a must for our society; most of the portable electronic devices we use in our daily life is powered by Li-ion cells. There are many types of Li-ion cells, depending on the application. Li-ion cells can be manufactured in different forms, size, capacities, voltages, and powers, etc. The demand for Li-ion cells increased significantly with the developments in the automotive industry. Many new electric vehicle models with impressive features are released to the market. There are a lot of reasons to buy electric vehicles. The governments are giving perks to EV owners such as free or inexpensive charging, lower transportation taxes, and no emission taxes. Many of the pioneer countries have announced that they are going to have some regulations to limit fuel-based vehicle production. The sales and the demand for EVs are growing day by day, and automotive companies making great investments to get their piece of the pie. Numerous incentives for hybrid and electric vehicles have been established by many governments and local administrations around the world in order to speed up the adoption of electric vehicles [7].

In order to support the adoption of EVs, the new car models should meet specific criteria in various fields such as range, acceleration, weight, cost, and safety. Most of the EV's use battery pack as the power source, a typical battery pack is formed by connecting smaller cells series and parallel. If the battery pack has more cells in parallel, the peak current and the energy storage capacity will be greater. So, the vehicle will have a longer range. Same applies for cells in series, more cells in series will result in higher pack voltage; thus, it can deliver high power with lower currents. So, the vehicle will have better acceleration. High voltage battery packs with great energy and power rates tend to use thousands of battery cells. To store higher energy in smaller weights, car manufacturers prefer higher WH/kg cells. Lithium-ion batteries have high energy storage densities and a clear advantage over other batteries for electrifying transportation, this makes them very preferable.

1.1 Purpose of Thesis

Battery Management Systems (BMS) are used to monitor lithium-ion battery packs. The BMS ensures that the pack stays in a safe operating range, controls its environment, and balances every cell. [6]. In order to operate the battery pack effectively, the available SOC must be calculated precisely by the BMS. But, this is not an easy task because there is no direct way to measure SOC, a robust estimation algorithm with a proper simulation model is needed to be employed.

The purpose of this thesis is to model the battery cells of a real HEV's and design a proper algorithm to estimate SOC for real-world application.

2. LITERATURE REVIEW

The definition of the battery can be given as the system which is able to convert chemical energy to electric energy by using electrochemical reactions. The first description of the batteries was made in an 1800 study by Volta, who is an Italian professor at the University of Pavia. He invented the voltaic pile in 1800, which is the first form of the battery as we know it today. Since its invention, considerable studies made and various battery chemistries have been developed [1].

2.1 General Operating Principles of Li-Ion Batteries

At the present time, batteries are categorized as primary and secondary batteries, primary batteries manufactured and stored with a full charge and they cannot be re-charged after the first usage, they should be disposed. On the other hand, secondary batteries are rechargeable; they can be used many times. Among all of the secondary battery chemistries, the lithium-ion one has clear advantages over all of the other types. Li-ion secondary batteries offer longer service life, higher energy density, and higher operating voltage. This thesis will focus on secondary batteries, particularly li-ion chemistry.

2.1.1 Lithium secondary batteries

An electrochemical cell uses reduction and oxidation (Redox) reactions to convert chemical energy to electric energy.

As it is illustrated in Figure 2.1, a lithium cell consists metal collectors named anode and cathode, they are placed in an electrolyte median and a separator plate to prevent a short circuit between the electrodes. When redox reaction takes place at the electrodes, ions are transferred through the electrolyte between the anode and the cathode. Electron transfer is needed between electrodes to equalize polarization, but electrons cannot transfer through electrolyte because of the separator. Instead, they

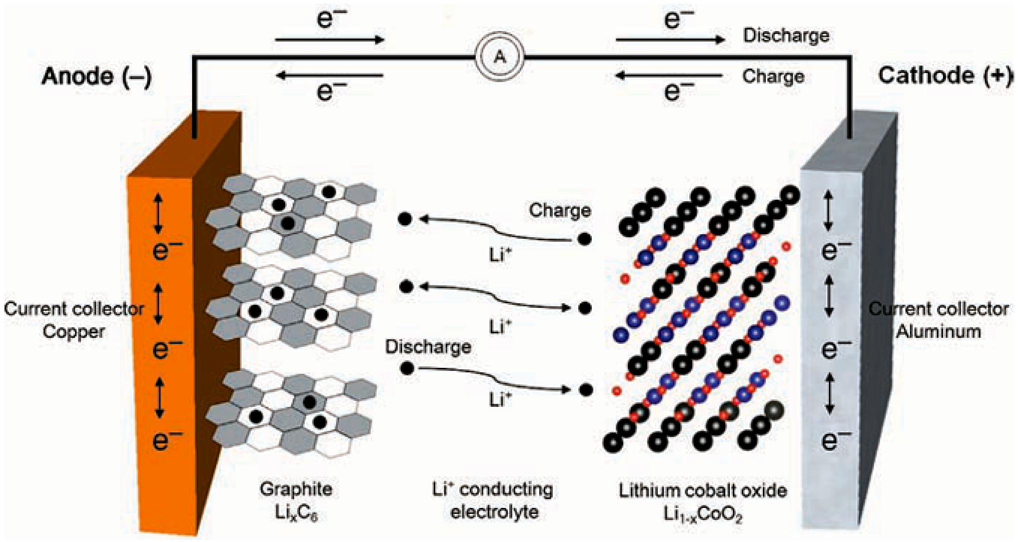

Figure 2.1 : Movement of Li^+ in an electrolyte in a battery. [1]

travel through an external wire connecting the two electrodes. If a load is connected to the terminals, the current will flow over the load, and power transfer is realized.

2.2 Terminologies and Definitions

2.2.1 Cells, modules, and packs

Most of the EV's use high voltage battery packs as the rechargeable energy storage system (RESS), a typical HV battery pack may use thousands of battery cells, to meet high energy and power requirements of the EV's. A Li-ion cell is the most fundamental element of the battery pack, and they usually provide 3-4 V. [8] By connecting many cells in parallel battery blocks are formed, and they provide same voltage with the cell, but they have higher capacities. By connecting battery blocks in series modules are made, modules have the same capacities as the blocks, but they provide higher voltages. Finally, the packs are built by connecting the battery modules. If the battery pack has more cells in series, it will have a higher pack voltage. Thus it will deliver and absorb higher powers with lower current, enabling the vehicle to have better acceleration and deceleration performance. Similarly, more cells in parallel will increase the energy storage capacity, resulting in the vehicle to have more extended range. Figure 2.3 shows an illustration of an EV battery pack consisting of many modules. Also, figure 2.2 shows that a module may use many cells.

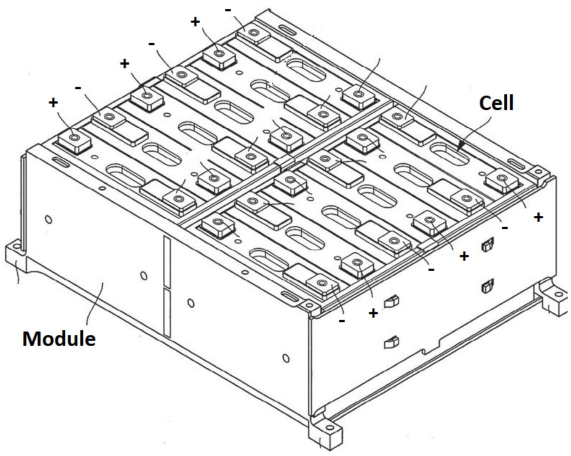

Figure 2.2 : Cell module with prismatic lithium-ion cells. [2]

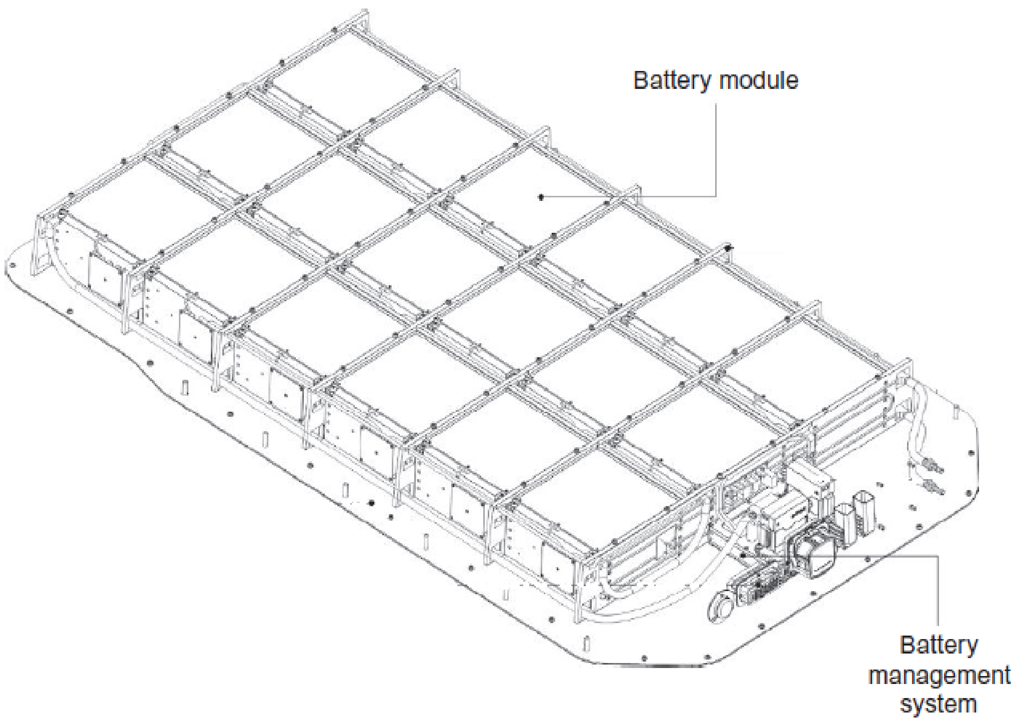

Figure 2.3 : A battery pack with lithium-ion modules for an EV . [2]

2.2.2 C-rate

The C-rate defines the speed a battery is discharged or charged. 1C is the current rate which a fully charged battery will consume all its usable energy in one hour. For a cell with the capacity of 50 Ah, 1C defines 50 Ampere, similarly for a 2Ah cell 1C is 2A. Different applications require different performance criterion, so while evaluating different cell candidates for an application, C-rate comes very handily. It will help users to decide if they should use one 50Ah cell or 25 2Ah cells in parallel.

2.2.3 Terminal and open-circuit voltages

The voltage measured between battery terminals when a current flow over the battery is called terminal voltage. On the other hand, open-circuit voltage (OCV) is the resting voltage of the battery, or steady-state voltage value when no current disturbance is applied to the battery. In this thesis, OCV is used as a function of State of Charge, temperature, and current direction [8].

2.2.4 Capacity

The capacity can be defined as, the electrical energy storage capability of a battery in ampere-hours (Ah). Capacity can be calculated by drawing a constant current from a fully charged battery until the end-of-discharge voltage is reached. The current times elapsed time will give capacity in Ah. Capacity can be changed due to C-rate, at higher charge/discharge current rates battery capacity is lower. At higher currents, the voltage dissipation tends to be greater; thus, end-of-discharge or end-of-charge voltages reached earlier.

2.2.5 State of charge (SOC)

Measuring the remaining fuel in conventional vehicles is very straightforward. A float connected to a potentiometer is placed in the fuel tank, as the fuel level goes down, the float decreases vertically and slides a moving contact along with the resistor, increasing its resistance. Then, by using a conversion table, this resistance value is mapped to the remaining liter, and the driver can be informed about how much fuel is left in the vehicle.

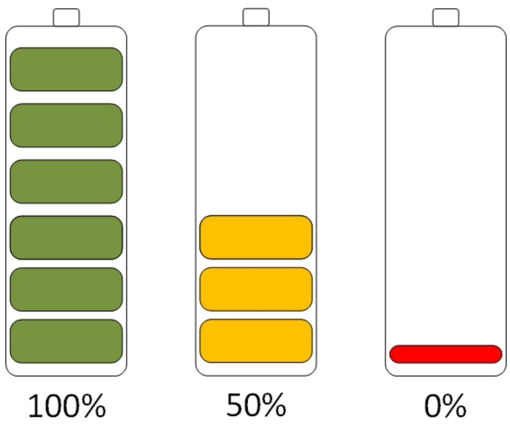

Figure 2.4 : State of charge illustration.

In the same manner, EV's use SOC to indicate remaining energy of the battery, an illustration is given in In figure 2.4. It can be expressed in percent; SOC is 0% when the battery is empty and, 100% when it is full. For the sake of longer life span, batteries are not used at their extreme voltage points. Instead, an optimum working voltage interval is determined, then 0% SOC is paired with the minimum OCV of the interval, and the maximum OCV is paired with 100%. The capacity of this interval is measured and fragmented equally. So, the SOC values of the same batteries at the same voltages may differ from application to application. There is no direct way to measure SOC; there are only indirect ways to estimate it, in this thesis numerous methods for estimating SOC will be given and specifically Extended Kalman Filter will be applied to real cell data.

2.2.6 Depth of discharge (DOD)

Depth of discharge is another way to keep track of the remaining energy of the battery. Simply, DOD is the measure of the charge removed from a battery in Ah or percentage. If it is expressed in percentage basically, DOD (%) = 100 – SOC(%). But in literature, it is stated that expressing DOD in Ah is more advantageous. The reason is when all of the charge is removed from the cell the SOC will be 0%, at this point if you were to remove more energy from the cell, the SOC value cannot go lower, only DOD(Ah) can continue to count removed energy. Same applies for overcharging, the SOC value cannot track values more than 100%, but DOD can be represented in negative values [6].

2.2.7 Cut-off voltage

This term is used to express extreme voltage points of the battery. A battery should not be discharged below the low cut-off voltage or charged above the high cut-off voltage. Otherwise, irreversible chemical reactions might occur, resulting in a and diminish battery health or even cause thermal runaway (destruction of the battery) [6].

2.2.8 Cycle life

In literature, it is assumed that the battery has reached its End of Life (EOL) when the capacity is reduced to 80% of the Beginning of Life (BOL) capacity. Cycle life is the number of fully discharge-charge cycles until the battery has reached its EOL. Cycle life strongly dependent on C-rate, temperature, and voltage window of the cycles. Higher C-rate, higher voltage window, and operating at extreme temperatures will reduce cycle life [6].

2.2.9 State of health (SOH)

During the lifetime of the battery, some irreversible chemical reactions take place resulting capacity to reduce, internal resistance to increase, etc., and the overall performance of the battery will reduce. Hence, an aging measure is needed to be employed in order to estimate the remaining useful lifetime (RUL) of the battery. Although, the state of health (SOH) is a definition may differ from manufacturer to manufacturer. It can be generalized as an arbitrary measure that allows comparing batteries present conditions with the beginning of life (BOL) conditions. Many of the works in literature uses only capacity reduction as the primary indicator of the SOH, but there is a considerable amount of works that also take account of the increment in internal resistance. [[9, 10]] Just like Operating outside of the suggested working conditions will damage the battery and accelerate aging effects resulting premature aging, some of the reasons can be listed as vicious currents cycles, extreme temperatures, overcharging, under-discharging, etc. [11, 12]

3. CELL MODELLING

The ultimate goal of this work is to achieve an accurate and robust estimation of SOC for a good BMS performance. This requires knowledge of battery cell parameters. In this chapter, the development of a precise battery simulation model will be demonstrated, and to increase the robustness of the model an EKF will be designed to estimate battery's SOC. In order to build a detailed simulation model, precise cell data was needed, so various test procedures in different temperatures were applied on 51Ah Li-ion NMC cells by using a battery test chamber. During test procedures data from various measurement points are recorded. Later on, the obtained test data is analyzed then used for acquiring equivalent circuit analogy in MATLAB and Simulink environments.

Cell modeling requires knowledge of battery cell parameters. To this aim first, the battery is modeled using an electrical circuit equivalent at the cell level, and then at the battery pack level. In order to model a battery cell, the equivalent circuit parameters and the Open Circuit Voltage (OCV) have to be determined. To this aim, we use the cell test data provided by a Li-ion cell manufacturer. First, the cell's Amp-H capacity (Q) is determined by discharging the cell with current pulses. Next, for each temperature value, using the Ampere Hour Counting method, the SOC of the cell is determined, and this is related to OCV values for each temperature. A MATLAB/Simulink based curve fitting is then implemented to obtain OCV as a function of SOC and temperature.

Next, the equivalent circuit parameters are determined. To this purpose, the Hybrid Pulse Power Characterization (HPPC) test is performed to obtain cell current, and voltage values for various temperatures and the associated SOC values are obtained. Then, the 2RC model of the battery cell is built on Simulink. Next, using the current values (of the HPPC table for each temperature value) as the input, and voltage values as the output, together with OCV values as a function of SOC, the equivalent circuit parameters are determined. At this point, obtained cell parameters are placed in the related locations in the battery's state space equations. Later, State Space form of the battery is used in the EKF developing process, by this way battery SOC can be determined in real time for any driving cycle using the Extended Kalman Filter (EKF). The commonly used Worldwide Harmonized Light Vehicle Test Procedure (WLTP) is considered for the validation driving cycle for EKF, the real SOC data is compared with the EKF SOC estimations.

After validating EKF, a battery pack simulation model is built by connecting 16 cells in series. Later on, a balancing mechanism which is controlled by the EKF estimations is added to the simulation model. At this stage of the study, dissipative shunt resistor balancing topology is modeled for the sake of simplicity, but other balancing topologies such as a switched capacitor, multi-winding transformer, full bridge converters, switch networks, etc. can easily be employed for future works.

3.1 Equivalent Circuit Modelling

The equivalent circuit model approach is highly accepted in many areas, adequate approximation of the battery model can be achieved with less computational effort than electro-chemical approximation. The circuit can be rather simple, e.g. only a voltage source and a variable resistance or complex, with additional variable resistances, capacitors and hysteresis to better capture the transient response. Simplicity and robustness of the equivalent circuit model approach allow these models to be implemented in real time applications. These models also can be coupled with thermal models to predict the overall cell behaviors like cell degradation, capacity fading, and power fading.

3.1.1 2RC model

To provide an acceptable representation for the battery behavior, 2 RC equivalent circuit model which reflects the behavior for two frequencies is selected. In figure 3.1, R0 is the battery internal resistance to simulate immediate changes in voltage according to current , R1-C1 and R2-C2 couples to capture capacitive behavior of the battery, and OCV to represent the battery's steady state voltage according to SOC. This model is able to capture fast and slow time constants for the voltage recovery of the battery.

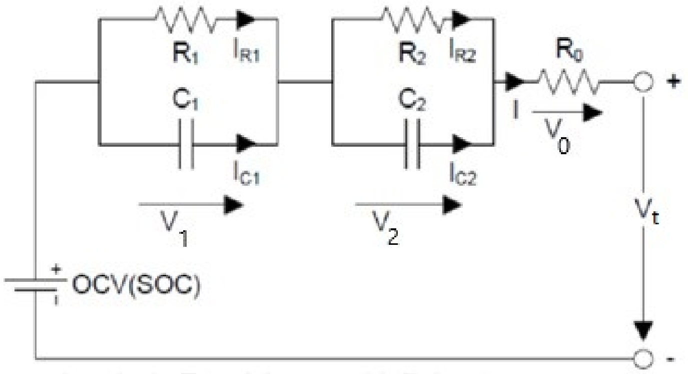

Figure 3.1 : Schematic diagram for R-RC-RC battery model [3].

The state-space representation of the 2RC cell model is as below.

$$SOC = SOC_0 - \frac{100}{3600} \int_0^t \frac{I(t)}{Q_c} dt \tag{3.1}$$

$$\frac{\mathrm{d}V_1}{\mathrm{d}t} = \frac{I}{C_1} - \frac{V_1}{C_1 R_1} \tag{3.2}$$

$$\frac{\mathrm{d}V_2}{\mathrm{d}t} = \frac{I}{C_2} - \frac{V_2}{C_2 R_2} \tag{3.3}$$

$$x = \begin{bmatrix} SOC & V_1 & V_2 \end{bmatrix}^T \tag{3.4}$$

$$\frac{\mathrm{d}}{\mathrm{dt}} \begin{bmatrix} SOC \\ V_1 \\ V_2 \end{bmatrix} = \begin{bmatrix} 0 & 0 & 0 \\ 0 & -1/R_1 C_1 & 0 \\ 0 & 0 & -1/R_2 C_2 \end{bmatrix} \begin{bmatrix} SOC \\ V_1 \\ V_2 \end{bmatrix} + \begin{bmatrix} -100/3600\, Q_c \\ 1/C_1 \\ 1/C_2 \end{bmatrix} I \tag{3.5}$$

$$V_t = OCV_{SOC} - R_0 I - V_1 - V_2 \tag{3.6}$$

Here, R_1C_1 are the fast polarization time constants, R_2C_2 are the slow polarization time constants,V_1 represents the voltage across the first capacitor, V_2 represents the voltage across the second capacitor.The current I is the only input, and terminal voltage V_t is the only output. The parameter vector to be estimated is $\theta = \begin{bmatrix} R_0 & R_1 & R_2 & C_1 & C_2 \end{bmatrix}$ Q_c: nominal capacity of a cell, measured in Ah. Capacity is 51 Ah for the model and varies with temperature.

The procedures for the determination of OCV as a function of SOC, temperature and current direction (hysteresis) is described below.

3.1.2 Derivation of OCV function

For this purpose, test data provided for various temperatures (-25°, 0°, 25°, 35°, 45°, 55° C) is used. Briefly, this test procedure is started with 100% SOC and conducted by reducing the SOC by steps of 5% at a constant temperature. Between each step, there should be a rest period before taking the voltage (OCV) reading to give the transients sufficient time to settle. The rest duration was 4 hours in this test. By repeating this test from 0% SOC to 100% SOC, it is possible to capture the well-known hysteresis effect. As a result, the OCV function is obtained as a function of SOC for constant temperature values and charge-discharge conditions, using the MATLAB Curve Fitting Toolbox.
For ease of demonstration, the OCV values during charging and discharging are given on separate axes, using a 3D representation. The lower OCV values at discharging support the expected hysteresis effect, which is also reflected in the derived OCV function.

3.1.2.1 OCV values during charge

The OCV data in this section is obtained in charging direction, so the SOC value is near to 0% at the starting of each experiment and charging current is applied to increase SOC with the steps of 5% until it reaches to 100%. 4 hours of resting time is given to the cells between each step, this way the true charging OCV values are recorded. This procedure is repeated for different temperatures and OCV values according to SOC is recorded.
Later, the collected OCV_{SOC} table for different temperatures are merged, and $OCV_{SOCTemp}$ table is obtained. With the help of MATLAB Curve Fitting Toolbox, this table is fitted to a function by using the Cubic Interpolation method. Smooth transition between OCV values is guaranteed this way, OCV_Ch = f (SOC, Temp) is plotted in Figure 3.2

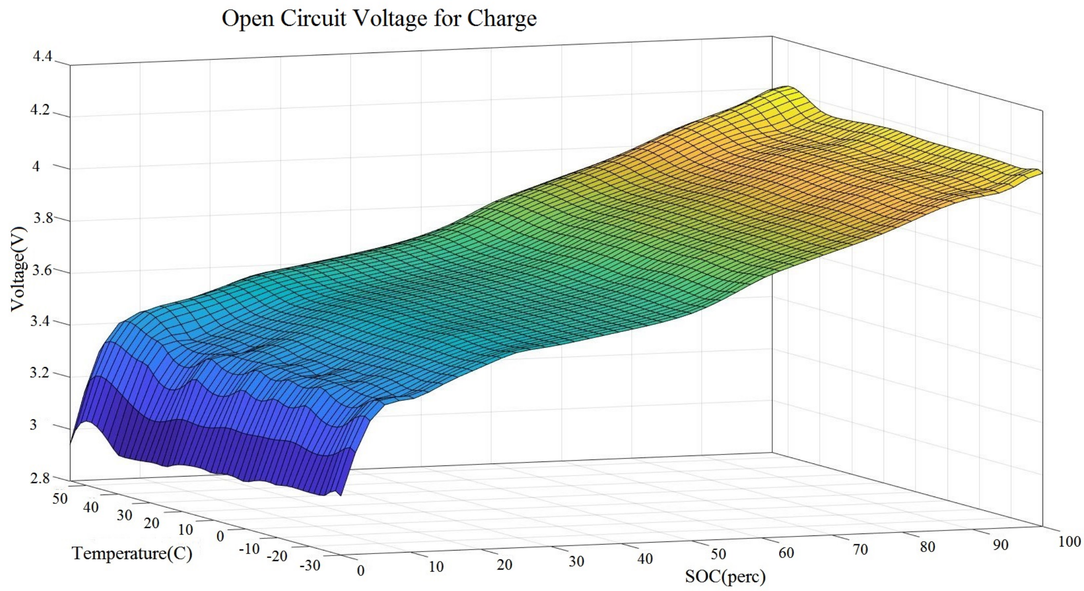

Figure 3.2 : OCV values with respect to SOC and temperature during charge.

3.1.2.2 OCV values during discharge

The OCV data in this section is obtained in discharging direction, so the SOC value is near to 100% at the starting of each experiment and current drawn from the battery to decrease SOC with the steps of 5% until it reaches to 0%. 4 hours of resting time is given to the cells between each step, this way the true discharging OCV values are recorded. This procedure is repeated for different temperatures and OCV values according to SOC is recorded.
After that, the collected OCV_{SOC} table at different temperatures are merged, and $OCV_{SOCTemp}$ table is obtained for discharging direction. This table is fitted to a function by using the same method applied to charge data. Smooth transition between OCV values is guaranteed this way, OCV_Dch = f (SOC,Temp) is plotted in the Figure 3.3.

The ultimate OCV function with the hysteresis effect is built by adding a switch logic between OCV_Ch and OCV_Dch functions. A moving average logic is used between switched values in order to provide smooth transition between charge and discharge OCV values.

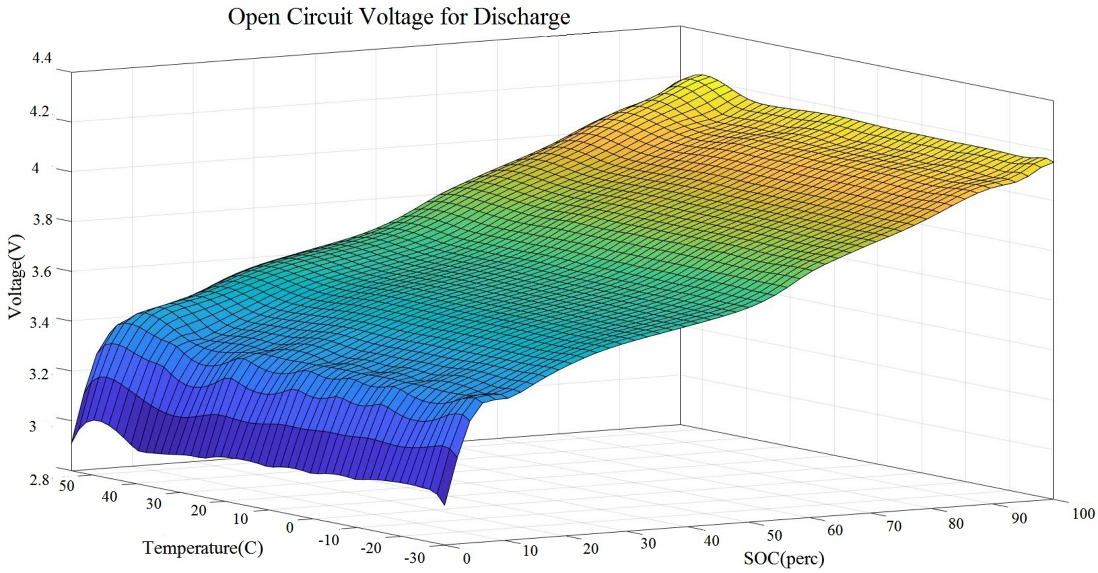

Figure 3.3 : OCV values with respect to SOC and temperature during discharge.

3.1.3 HPPC test

The HPPC test could be described as a procedure of drawing current pulses from a battery cell to capture terminal voltage changes based on the current waveform at different temperatures. Figure 3.4 is an example for the HPPC test profile.

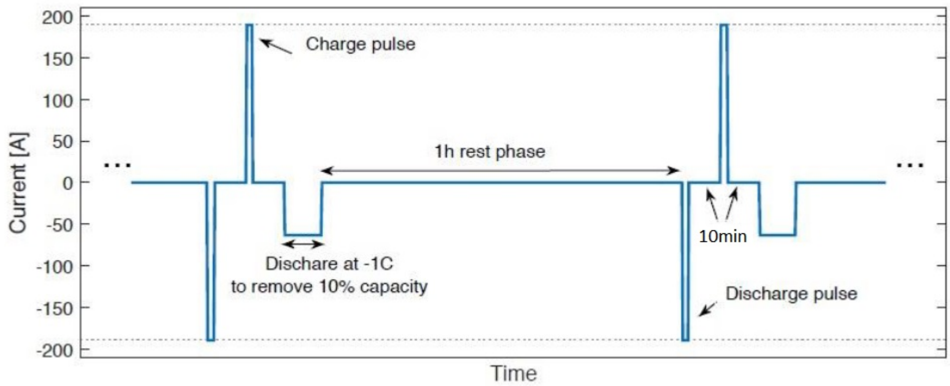

Figure 3.4 : HPPC test profile sample.

The procedure explained above is applied to the 51 Ah NMC test cells at various temperature and SOC values. The summary of the HPPC tests can be seen in Table 3.1. Net discharging capacities are smaller at lower temperatures, and test cycle times are longer.

Real time measurement data of current and voltage values during HPPC tests are given in the following sections

Table 3.1 : HPPC Test Summary.

Temperature (C)	Cycle time (s)	Discharging (Ah)	Charging (Ah)	Net discharging(Ah)
40	24871	48.37	3.51	44.86
25	29258	47.96	3.63	43.33
0	31704	41.25	0.84	40.41
-20	30314	37.16	0.21	36.95

3.1.3.1 HPPC test results at T= 40° C

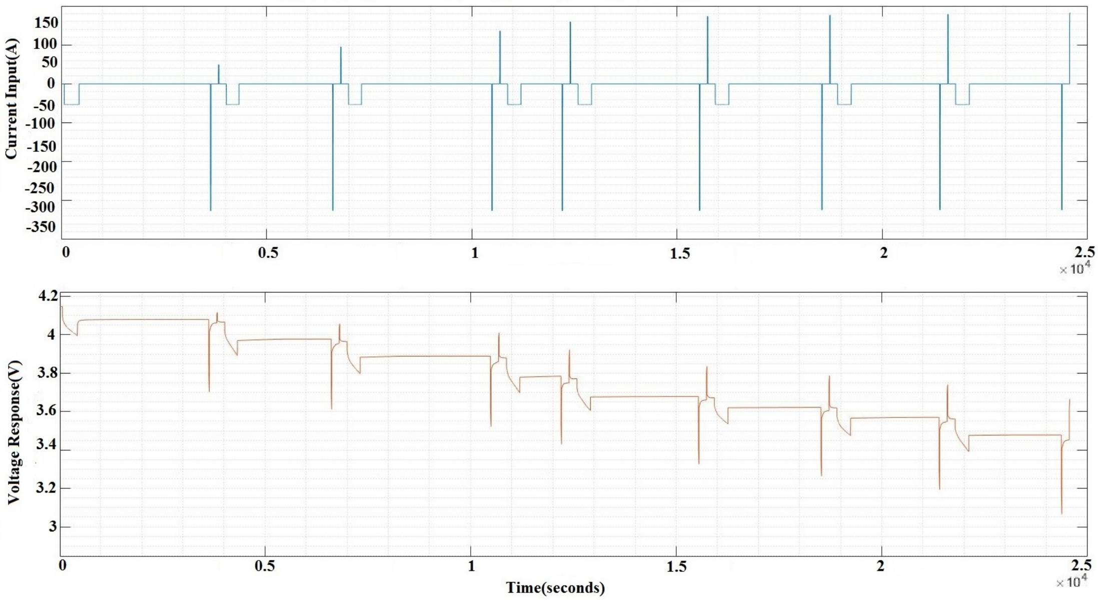

Figure 3.5 : HPPC test data at T= 40° C.

3.1.3.2 HPPC test results at T=25° C

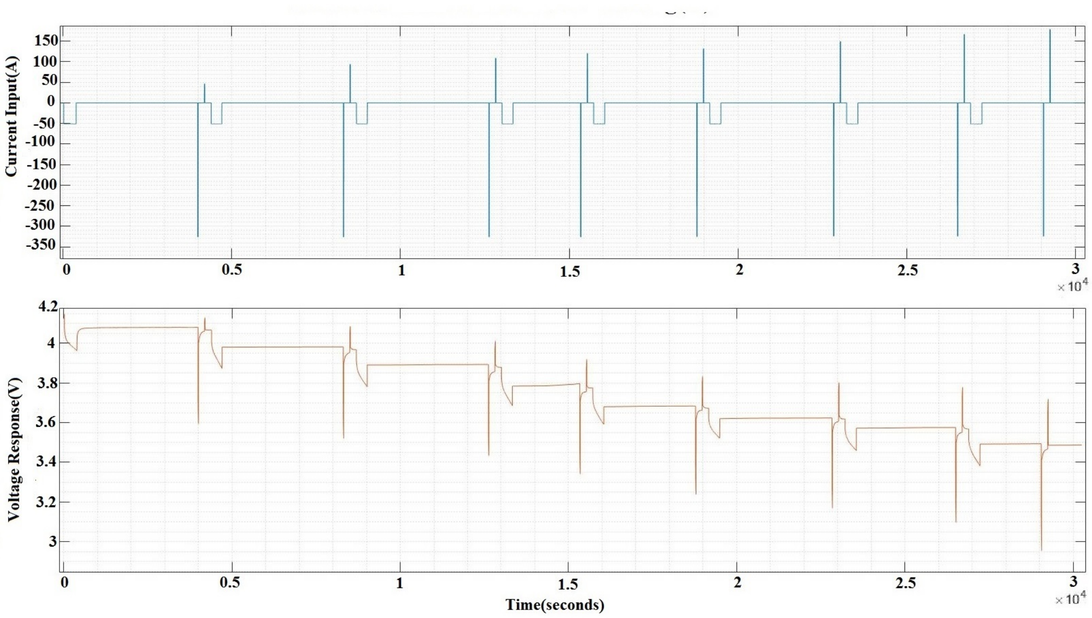

Figure 3.6 : HPPC test data at T= 25° C.

3.1.3.3 HPPC test results at T= 0° C

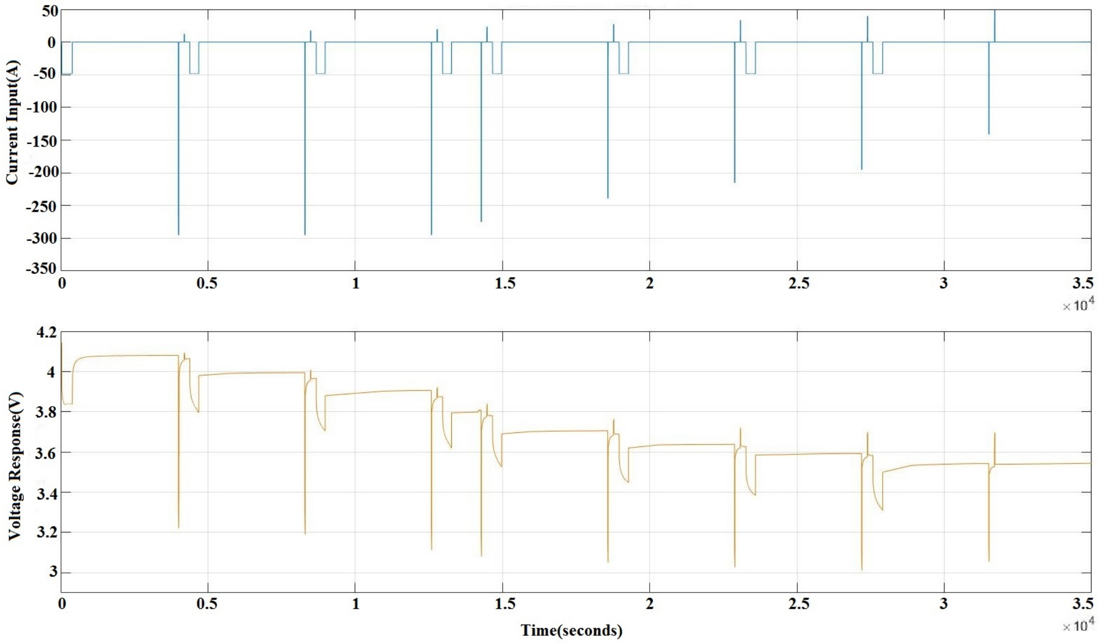

Figure 3.7 : HPPC test data at T= 0° C.

3.1.3.4 HPPC test results at T= -20° C

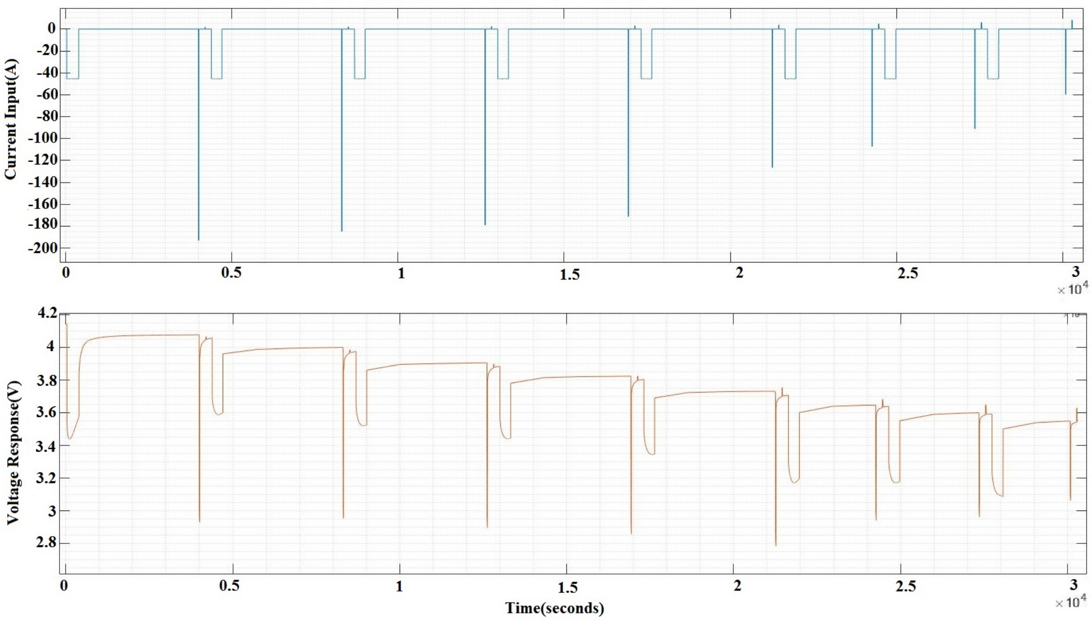

Figure 3.8 : HPPC test data at T= -20° C.

It can be seen that the applied currents are different for different temperature values. This is because deliverable power and charging power is dependent on temperature; e.g. at T= 25° C the battery can be charged and discharged with a very high powers but at T= -20° C even a small charge current can damage the cell. Hence, the terminal voltage profile changes with temperature.

Utilizing the OCV= f (SOC, T) from before, and taking cell voltage readings from the HPPC test at different temperature, the battery cell equivalent parameters are obtained via the 2RC model in Simulink.

3.1.4 Parameter determination

To determine the circuit parameters, the HPPC tests given above are used as training data. Notice that the temperatures kept stable for individual tests, thanks to climate control of battery testing chamber. This enables us to relate RC parameters purely with SOC values at constant temperatures. The load currents applied in the form of pulses, SOC values monitored with the help of Ampere-hour counting, obtained SOC values given as an input to the RC parameters. Below is a description of the test, application of current pulses, and the resulting determination of SOC (which is then related to the OCV through the above obtained OCV= f (SOC) values, and ultimately that of the circuit parameters.

3.1.4.1 2RC Simulink model

Figure 3.9 is created in Simulink environment. The Capacity and OCV_{SOC} are the known parameters from OCV and Capacity Test results. R0, R1, R2, C1, and C2 are the parameters to be estimated. At the initial state, the parameters are assigned random initial values; then they are corrected by Simulink Parameter Estimation Toolbox.

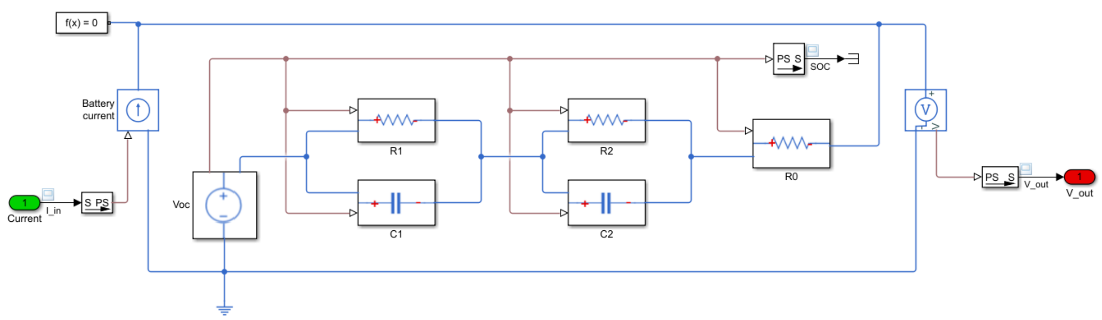

Figure 3.9 : 2RC Simulink model for parameter estimation.

3.1.4.2 Simulink parameter estimation toolbox

With the help of this toolbox, HPPC Test data is associated with the 2RC Simulink Model. The HPPC test data includes real-time voltage responses to the current pulses applied to the battery (to derive a constantly decreasing profile for SOC). Using these input-output values, the equivalent battery resistances and capacitors are calculated iteratively by the simulation program.

Figure 3.10 demonstrates the results of the first iteration step. As can be seen in the beginning iterations for the estimation of R0, R1, R2, C1, C2, the battery voltage calculated with the estimated circuit values deviates significantly from the actual measured battery cell voltage, but this deviation decreases at the end of iterations.

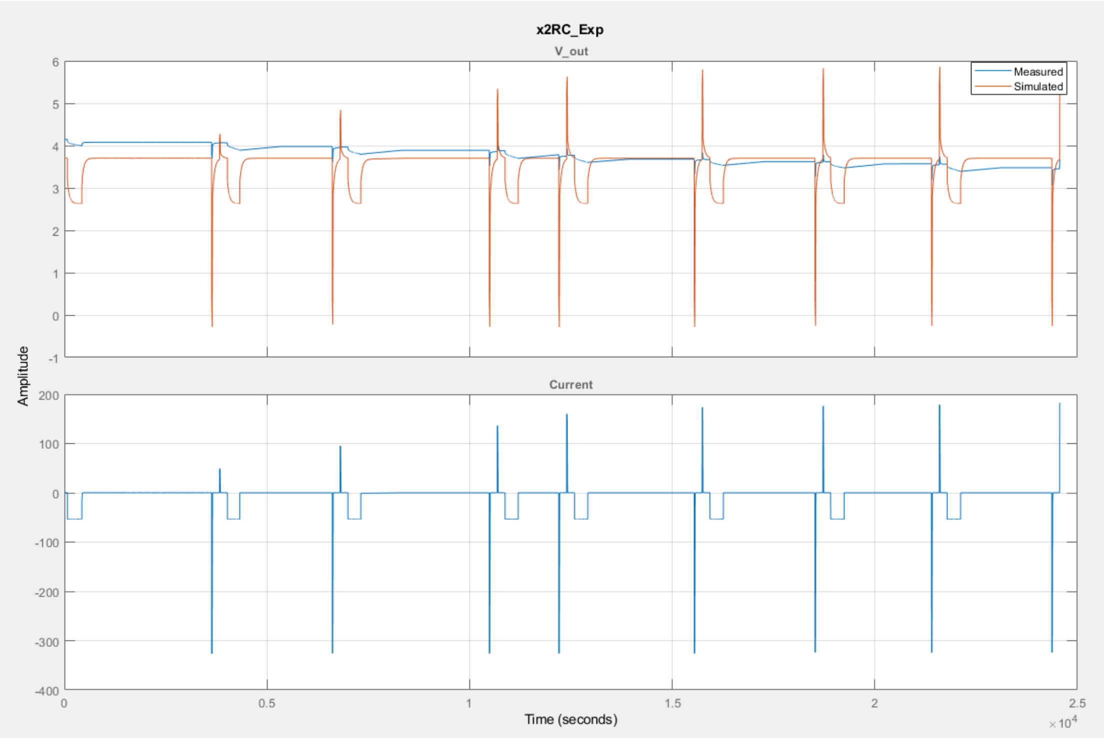

Figure 3.10 : Initial phase of parameter estimation where simulated and measured voltages are different.

At the end of parameter estimation session, the RC parameters corrected by the Toolbox, resulting with measured and simulated terminal voltages are matched almost entirely, in the Figure 3.11, i.e. the Sum of Squared Error is lower than 0.2%. So, one can conclude that the behavior 2RC equivalent circuit is very close to the actual battery cells.

This estimation procedure is applied for finding RC parameters for the following temperature values, T= -20°, 0°, 25°, 40° C. The RC parameters for different temperatures are gathered in excel form, and curve fitted to provide the interpolated values as needed for all temperature values in the operation range.

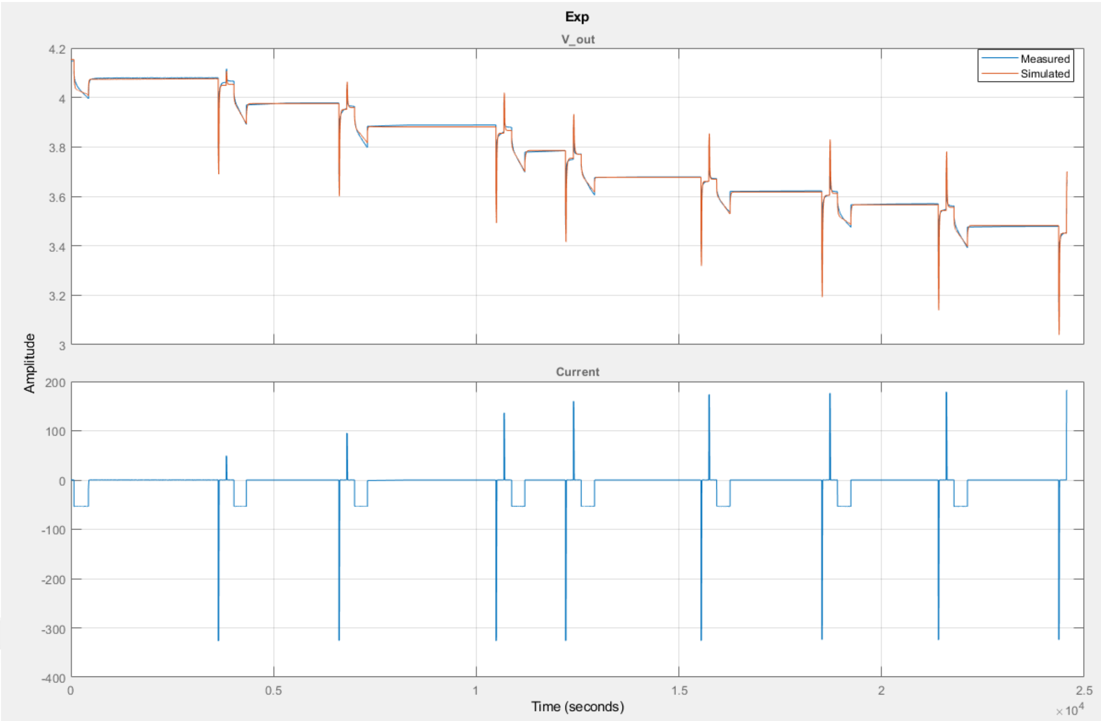

Figure 3.11 : Final phase of parameter estimation where simulation voltages converged to measurement.

In short,

• MATLAB Curve Fitting Toolbox is used for gathering RC parameters at different temperatures (-20°, 0°, 25°, 40° C). As a result, RC parameters are found as a function of SOC and temperature.

• Cell model is built with derived RC, OCV and capacity parameters.

• Cell model is validated by WLTP (to be described below) test data taken from the test vehicle.

3.1.5 Complete cell model

The cell model is created by using the derived parameters from HPPC tests above at different temperatures and test results and using the real life Worldwide Harmonized Light Vehicle Test Procedure (WLTP) data. The complete model consists of four submodels; those submodels reproduce SOC, open circuit voltage, internal resistance, and dynamic voltage. The OCV submodel is dependent on SOC submodel output, and dynamic voltage submodel dependent on internal resistance model output.WLTP is a commonly used vehicle test procedure, based on a velocity profile. While it is commonly used for emission testing, it has also become the widely used test cycle for EV's and their batteries.

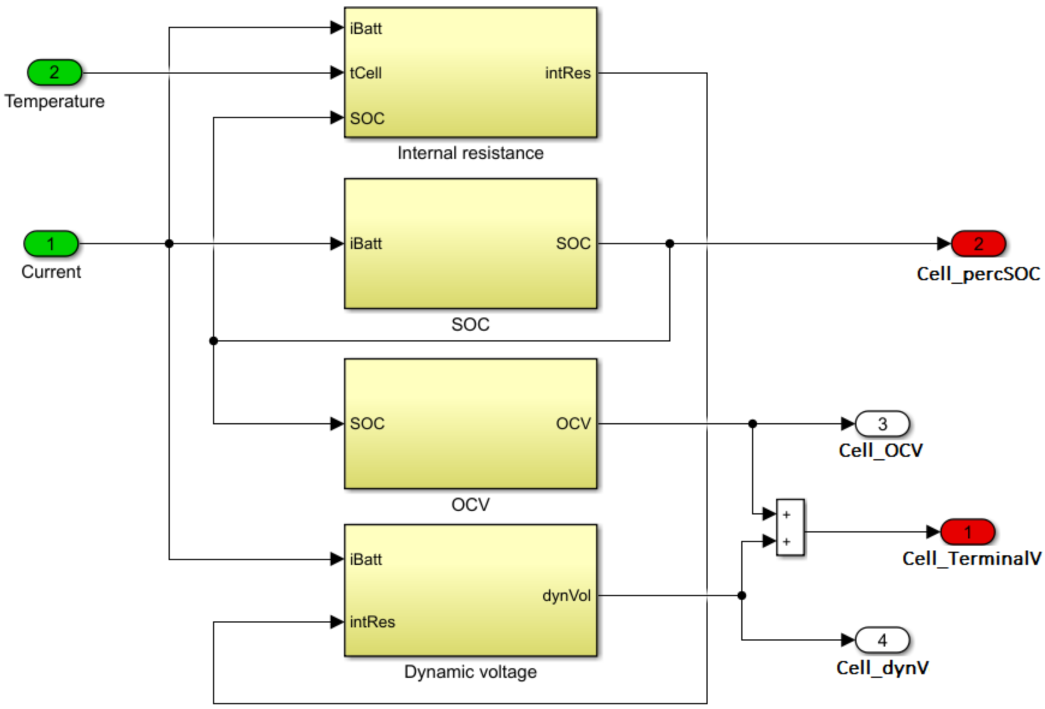

Figure 3.12 : Detailed battery cell model in Simulink.

3.2 Cell Model Validation

So far, the battery cell parameters derived by using the HPPC test data collected from the vehicle. In order to gain confidence about the model, simulation results must be compared with real-world measurements from the test vehicle. In this section the estimated parameters and the derived cell model will be validated using the worldwide harmonized light vehicles test procedure (WLTP). In order to validate proposed cell model, same inputs will be applied to the cell model and model outputs will be compared with real-time vehicle measurements. The inputs to the cell model are temperature, and current and the outputs are cell voltage and SOC. The validation values are satisfactory.

3.2.1 WLTP test

Worldwide Harmonized Light Vehicles Test Procedure is a new, realistic measuring process for determining a vehicle's range, fuel consumption, and emissions. The WLTP is valid as of 1 September 2018, for newly produced vehicles, it is obligatory for all EOM's and will be binding in all participating countries. The existing NEDC procedure developed in the 1990s and it inadequate regulate new vehicles; hence it is replaced with WLTP aiming new measurements mean a more precise, more comprehensible test result for every single car. [13]

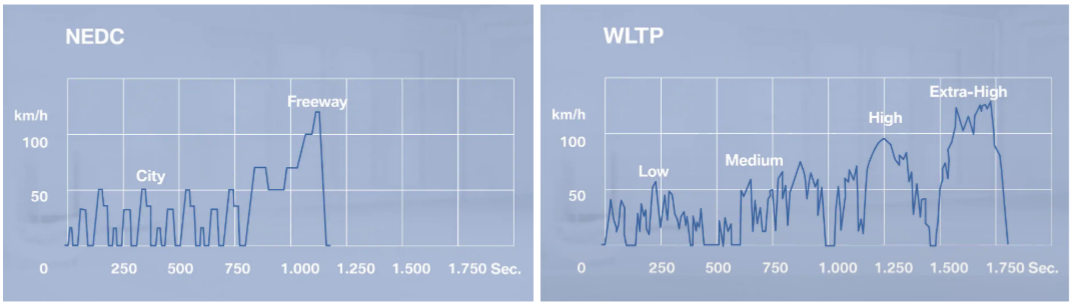

Figure 3.13 : Comparison between two test cycles NEDC and WLTP [4]

The difference between NEDC and WLTP cycles can be seen in Figure 3.13 , it is easy to say that clean and stable speed profiles of the NEDC are far from real-world driving cycles, while the WLTP offers more dynamic profile. In addition to that, while NEDC has only city and freeway modes, WLTP cycle includes low, medium, high and extra-high speeds making is closer to real-world driving profile [14] [15].

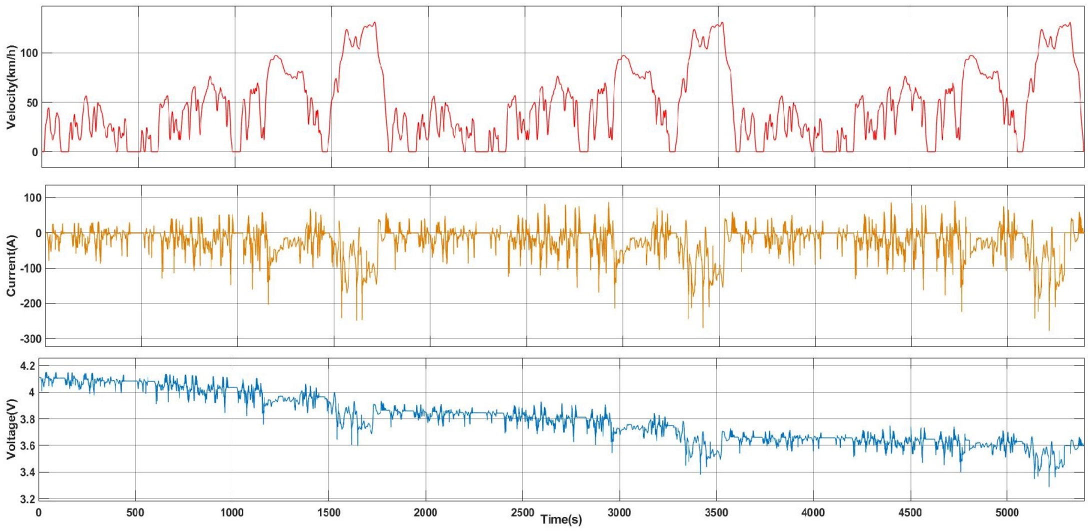

Figure 3.14 : WLTP test measurements from test vehicle.

The WLTP data from the test vehicle is shown in Figure 3.14. In this data WLTP profile is applied three times to the test vehicle; current, temperature and voltage values of each cell is recorded. Notice that WLTP is a speed profile; drawn current for accelerating an EV may change due to of its weight, so it is essential to optimize vehicle weight. during testing This data is utilized for model validation in the following subsection.

3.2.2 Simulation results

The modeling process is based on a best-fit of the recorded data from HPPC test, while the validation is made by comparing measured and simulated battery voltages of a different battery load cycle, which is WLTP test.

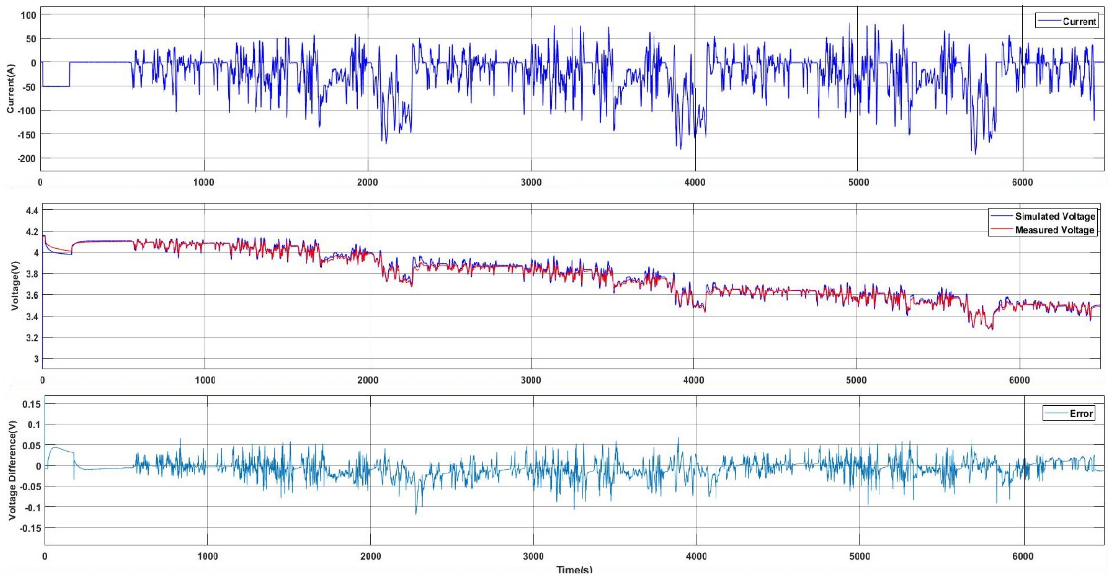

Figure 3.15 : Simulation results versus measurements.

As one can see in Figure 3.15 maximum deviation from the measurements is below 0.1 V and average error is about 0.03 V, this shows that transient behavior of the cell is captured with the accuracy of 1%. The comparison between simulations and measurements confirms that this model is capable of reproducing the real-world behavior of the battery accurately, presenting a proper approach for battery model design and optimization to the scientific community.

4. SOC ESTIMATION

Now that we gained confidence in the battery model, we can start the developing process of the state estimator design for SOC. In the laboratory environment, measurement noises can be minimized, but in real-life applications, most of the sensors suffer from measurement noises and discretization errors such as current and voltage sensors. Also, the starting SOC may not be certain in real-life applications; thus, a self-correction estimation algorithm needs to be employed to calculate SOC precisely [3].

4.1 Extended Kalman Filter

Among the many methods used for estimating the batteries' SOC, the Extended Kalman Filter (EKF) stands out due to its the fundamental predictor-corrector mechanism, which makes the filter robust to various modeling deficiencies like poor initialization or noise [3]. This section presents a step-by-step design the method of such a filter, based on a 2nd order Thévenin battery ECM. The noble performance of the EKF is verified against the battery model obtained in the previous section.

4.1.1 State space modeling

The designing process of the EKF start with state-space modeling of the system, later on, linearization of the state space model is necessary because Kalman Filter is designed to work on linear systems.

The second-order Thevenin equivalent circuit model is shown in Figure 4.1. The battery model is built by an OCV source, series resistance, and two resistor-capacitor networks in the series. The value of OCV is nonlinear and dependent on the SOC. The series resistance (R0) represents the internal resistance of the battery, whereas the RC parallel networks (R1, R2, C1, C2) reproduce the immediate response of battery voltage. The equations obtained in the subsection 3.1.1 at the page 11 will be linearized

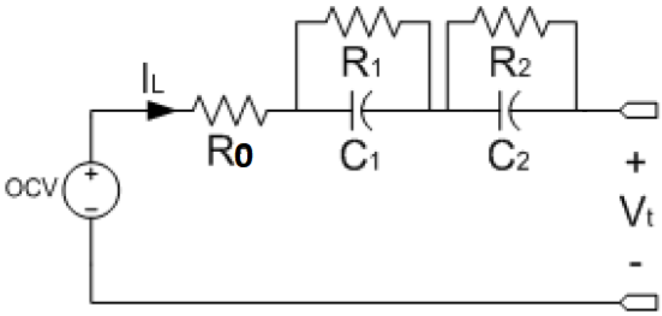

Figure 4.1 : Second order Thevenin equivalent circuit model.

as below. Generally, a non-linear system is described by the state-space model given in Eqns. 4.1 and 4.2.

$$x_{k+1} = f(x_k, u_k) + w_k \tag{4.1}$$

$$y_k = g(x_k, u_k) + v_k \tag{4.2}$$

$$w_k \sim N(0, Q), v_k \sim N(0, R) \tag{4.3}$$

Equation 4.1 is called the state equation, whereas eqn. 4.2 is the output equation. Here, k is the discrete-time index and x_k is the non-linear state vector. The system input is u_k , and wk is the white process noise with the covariance of Q, which represents some unmeasured input. The system output is y_k , and v_k is the discrete-time sensor noise with the covariance of R which directly affects the measurement of the output. The state transitions in Eqns. 4.1 and 4.2 are linearized about each sample point by Taylor series expansion trimming the terms higher than the second order. The resulting equations are given in Eq. 4.4.

$$x_{k+1} = A_k x_k + B_k u_k + w_k \tag{4.4}$$

$$y_k = C_k x_k + D_k u_k + v_k \tag{4.5}$$

The Jacobian matrices of the first order Taylor expansion are mathematically expressed in 4.6 - 4.9, where A_k, C_k are the first partial derivative matrices of f and g with respect to x_k ; and B_k, D_k are the Jacobians of the f and g functions with respect to u_k.

$$A_k = \frac{\partial f(x_k,u_k))}{\partial x_k} = \begin{bmatrix} 1 & 0 & 0 \\ 0 & 1-\dfrac{\Delta t}{R_1 C_1} & 0 \\ 0 & 0 & 1-\dfrac{\Delta t}{R_2 C_2} \end{bmatrix} \tag{4.6}$$

$$B_k = \frac{\partial f(x_k,u_k))}{\partial u_k} = \begin{bmatrix} \dfrac{-100\,\Delta t}{3600\,Q_c} & 1/C_1 & 1/C_2 \end{bmatrix}^T \tag{4.7}$$

$$C_k = \frac{\partial g(x_k,u_k))}{\partial x_k} = \begin{bmatrix} \dfrac{\partial OCV}{\partial SOC} & -1 & -1 \end{bmatrix} \tag{4.8}$$

$$D_k = \frac{\partial g(x_k,u_k))}{\partial u_k} = [-R_0] \tag{4.9}$$

The equations 3.5 and 3.6 are transformed to the equations below (4.10,4.11)

$$\begin{bmatrix} SOC_k \\ V_{1\,k} \\ V_{2\,k} \end{bmatrix} = \begin{bmatrix} 1 & 0 & 0 \\ 0 & 1-\dfrac{\Delta t}{R_1 C_1} & 0 \\ 0 & 0 & 1-\dfrac{\Delta t}{R_2 C_2} \end{bmatrix} \begin{bmatrix} SOC_{k-1} \\ V_{1\,k-1} \\ V_{2\,k-1} \end{bmatrix} + \begin{bmatrix} \dfrac{-100\,\Delta t}{3600\,Q_c} \\ \Delta t/C_1 \\ \Delta t/C_2 \end{bmatrix} I_{k-1} \tag{4.10}$$

$$V_{t_k} = \begin{bmatrix} \dfrac{\partial OCV}{\partial SOC} & -1 & -1 \end{bmatrix} \begin{bmatrix} SOC_k \\ V_{1\,k} \\ V_{2\,k} \end{bmatrix} + [-R0] I_k \tag{4.11}$$

The state-space equations of the battery given in Eqs. 4.10 and 4.11 are utilized to design EKF.

4.1.2 Steps of the algorithm

The generalized flow chart of the EKF is given in Figure 4.2.As It can be seen in the figure, the EKF algorithm utilizes experimental test data such as OCV tests, HPPC tests, and capacity tests. Battery model parameters found in chapter 3 are used for this purpose.

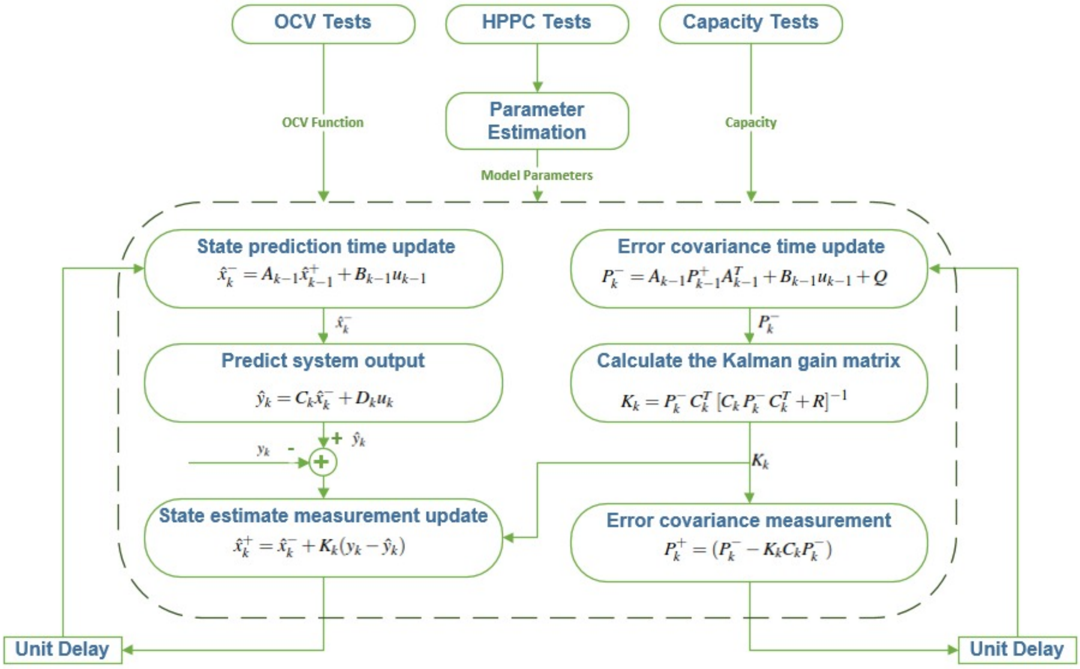

Figure 4.2 : The generalized flowchart of the EKF [5].

The initialization step of EKF is as in eq. 4.12, where P is the error covariance matrix related to the approximation of x [16].

$$k = 0 \tag{4.12}$$

$$\hat{x}_0^+ = E[x_0] \tag{4.13}$$

$$P_0^+ = E[(x_0 - \hat{x}_0^+)(x_0 - \hat{x}_0^+)^T] \tag{4.14}$$

The EKF process can be divided into two parts

1.The state estimate : The computation of best estimation for the present state value, which is $\hat{x}_k^+$

2.The covariance estimate : The computation of P_k^+ which is the uncertainty of $\hat{x}_k^+$, to be used to calculate error bounds [16].

Each part has three steps; steps of Extended Kalman Process are given in Eqns. 4.15 - 4.20

Step 1-a : State prediction time update.

$$\hat{x}_k^- = A_{k-1}\hat{x}_{k-1}^+ + B_{k-1}u_{k-1} \tag{4.15}$$

Computation of an updated prediction of the present value ofx_k, utilizing prior information on the system model. Here, $\hat{x}_k^-$ predicted state estimate at time index k(computed before measurement), and $\hat{x}_{k-1}^+$ is optimized state estimate at time index k-1(computed after measurement) [16, 17].

Step 1-b : Error covariance time update.

$$P_k^- = A_{k-1}P_{k-1}^+ A_{k-1}^T + B_{k-1}u_{k-1} + Q \tag{4.16}$$

Here, P_k^- predicted error covariance at time index k(computed before measurement) whereas P_{k-1}^+ is optimized error covariance at time index k-1(computed after measurement).

Step 1-c : Predict system output y_k.

$$\hat{y}_k = C_k\hat{x}_k^- + D_k u_k \tag{4.17}$$

$\hat{y}_k$ is the best estimation of the system output, and it will be used to calculate the optimized state estimate $\hat{x}_k^+$

Step 2-a : Calculate the Kalman gain matrix K_k.

$$K_k = P_k^- C_k^T \, [C_k P_k^- C_k^T + R]^{-1} \tag{4.18}$$

Step 2-b : State estimate measurement update.

$$\hat{x}_k^+ = \hat{x}_k^- + K_k(y_k - \hat{y}_k) \tag{4.19}$$

This step optimizes the predicted state estimate $\hat{x}_k^-$ by utilizing Kalman gain(K_k) and output prediction error($y_k - \hat{y}_k$)

Step 2-c : Error covariance measurement update P_k^+.

$$P_k^+ = (P_k^- - K_k C_k P_k^-) \tag{4.20}$$

The last step of the EKF process is updating error covariance matrix(P_k^-) by using Kalman gain K_k and the coupling term between state and output C_k. The resulting term P_k^+ will be used in the next iteration.

In the next section, the Simulink implementation will be given, and the validation process with simulation results to be stated.

4.1.3 Simulink implementation

The procedure explained in section 4.1 is simulated in MATLAB-Simulink environment. The inputs to the model are current, voltage, temperature, and capacity; the sampling time Δt is selected as 0.1 s. SOC predictions are saturated between -1.5 and 102 to eliminate irrational overshoot at the initialization.

The main output of the system is estimated SOC, but $V_1, V_2, and V_t$ estimations are also given as outputs for analyzing inner dynamics. The optimized process error covariance matrix and state estimations are given to the system as the feedback with the delay of one sampling time.

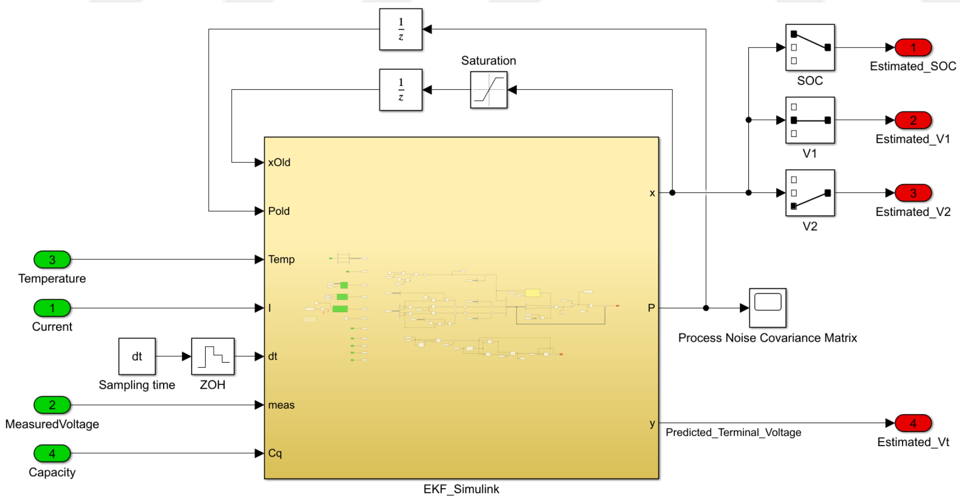

Figure 4.3 : EKF model in Simulink.

4.1.4 Simulation results

4.1.4.1 Validation with cell model

In this section, the figure 4.4 shows that EKF estimates are almost perfectly matched with the real states.

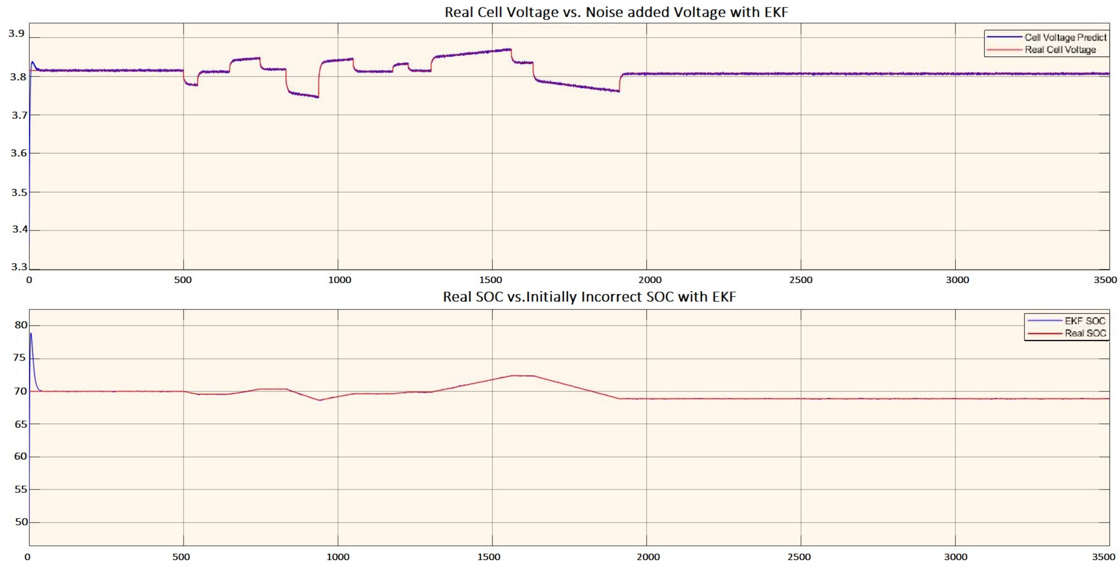

Figure 4.4 : Cell voltage and SOC estimation via EKF.

The SOC correction can be seen easily in the zoomed-in figure 4.5. The real SOC was 70% at the beginning, but EKF's initial SOC was 50%. Hence, although the EKF is started with 20% error, this is compensated in 25 seconds.

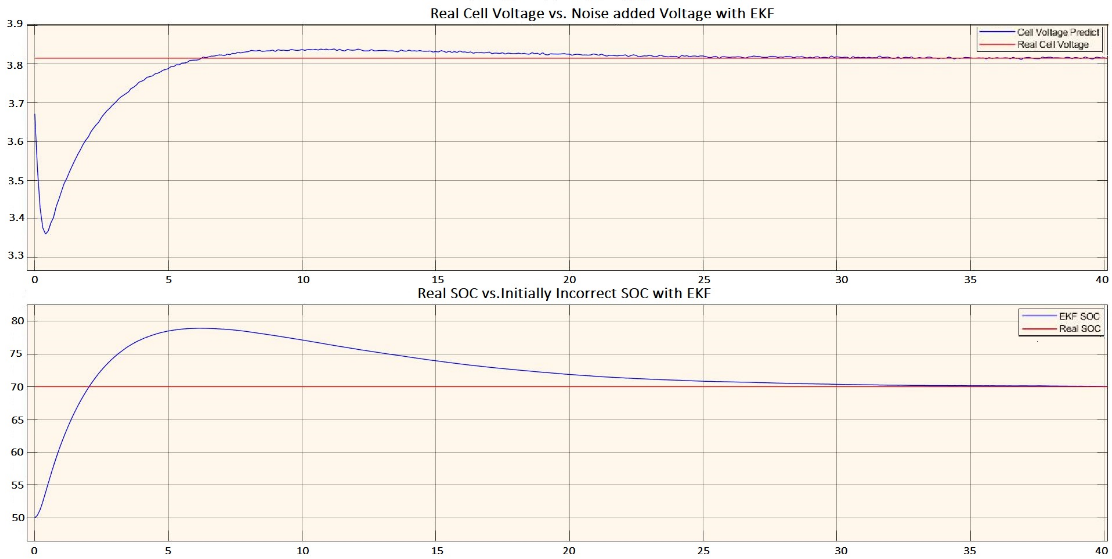

Figure 4.5 : EKF SOC correction when initialized with wrong SOC value.

4.1.4.2 Validation with real-life WLTP measurements

In the previous step, the developed EKF algorithm validated with the cell model. Now that we gain confidence about the EKF, we can observe the real-time behavior by connecting the real-life WLTP measurements from the test dynamometer. Measurements and EKF predictions can be seen in Figure 4.6 The Validation process is similar to the previous step, but this time, the real-life WLTP measurements from subsection 3.2.2 are used.

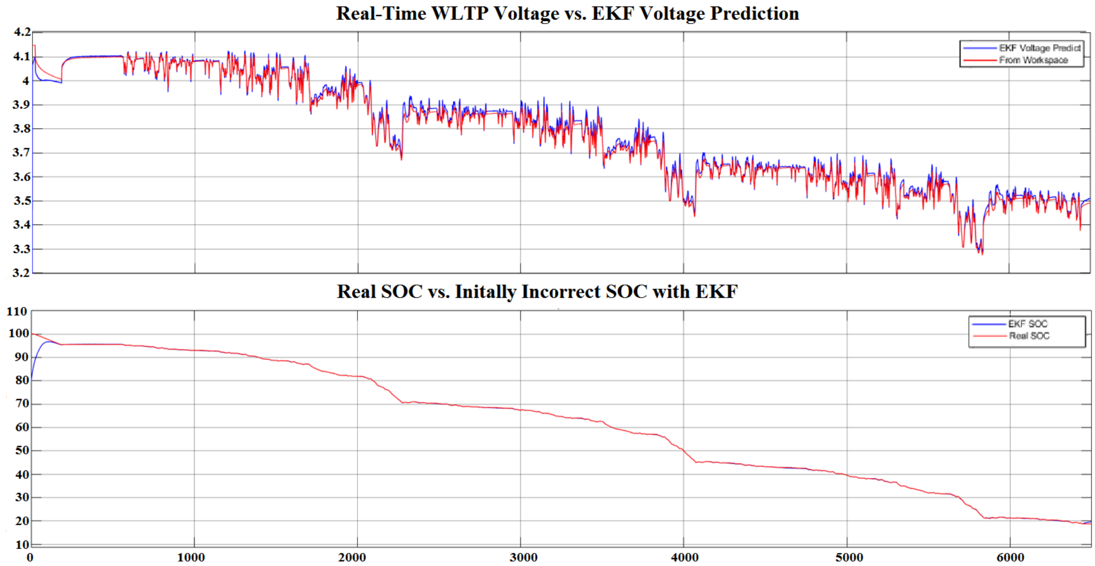

Figure 4.6 : EKF under real life WLTP measurements with 20% SOC initialization error.

Remember that in subsection 3.2.2, the initial SOC's of the real cells have to be known to achieve proper simulation results. But with the help of the designed EKF, wrongly initialized SOC value converged to the real SOC value in a short time. The corrective behavior can be seen in Figure 4.7

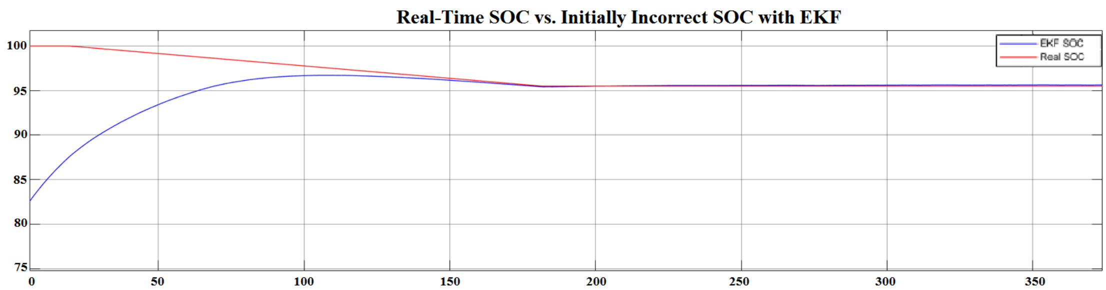

Figure 4.7 : Corrective behavior of EKF.

5. BATTERY PACK MODELING

A battery pack model is created in Simulink for 16 cells. Voltage and current sensors are added to each cell. With the pack model battery balancing also becomes an issue, which is known as the voltage discrepancies between each cells resulting in major failures both in charging and discharging. The following steps were conducted for charging, discharging and balancing.

Charging

Constant Current-Constant Voltage (CCCV) charger model is added to pack-level

Discharging

Discharge current profiles such as WLTP and HPPC are added to a signal builder

Balancing

A bleeding resistor (the resistor to remove the excessive charge from cells separately), a diode and a logical gate (MOSFET) are added to each cell to create a balancing mechanism. At this step, the passive balancing strategy is selected for the sake of simplicity. The passive balancing algorithm is implemented by controlling the logical gates of the bleeding resistors. The principle of this algorithm is to remove the excessive charge from the individual cells via bleeding resistors. To test the balancing mechanism, the cells are initialized at random SOC's and the balancing mechanism is tested during resting, charging, and discharging.

5.1 Application of This Study

In this section, the battery pack simulations are performed. First of all, 16 cells are connected serially in order to create a 57.6 V battery pack. Typically, characteristics of the serially connected cells are very similar, but even the slightest difference in the internal resistances, capacities or leakage (self-discharge current) leads to imbalance over time. This is a severe problem that needs to be addressed. The problem arises due to all of the cells being connected in series. As a result, the same current flows through all of the cells, whether it is charging or discharging. Hence, if one of the cells in series is at full charge, the charging current is commanded to be zero by the BMS to avoid overcharging. The same applies for discharging; i.e., if one cell is empty discharging must be stopped. Unbalance between cells prevents to use the remaining capacity of all cells and results in reduced battery capacities. Therefore, a balancing mechanism is essential to keep cells' charge at the same level [18].

Balancing during charging is illustrated in Figure 5.1 can be used. At the initial state, (a) second cell of the string is 4.1 volts, while others are around 3.5 volts. So, when the charge current is applied, the second cell reaches full charge much faster than the other cells, (b) charge process is stopped with the command from BMS, without the other three cells reaching full charge. The excessive charge should be removed via bleeding resistors; the balancing algorithm controls this. Once the excessive charge is removed, (c) the charging process can continue safely. After some time, (d) the second and fourth cells reach full charge, so the charging is stopped once again to remove the excessive charge. This process is repeated (e) until all of the cells are fully charged. At the final state, (f), it can be seen that all of the voltages have reached 4.2 V, and the charging process can be terminated [6].

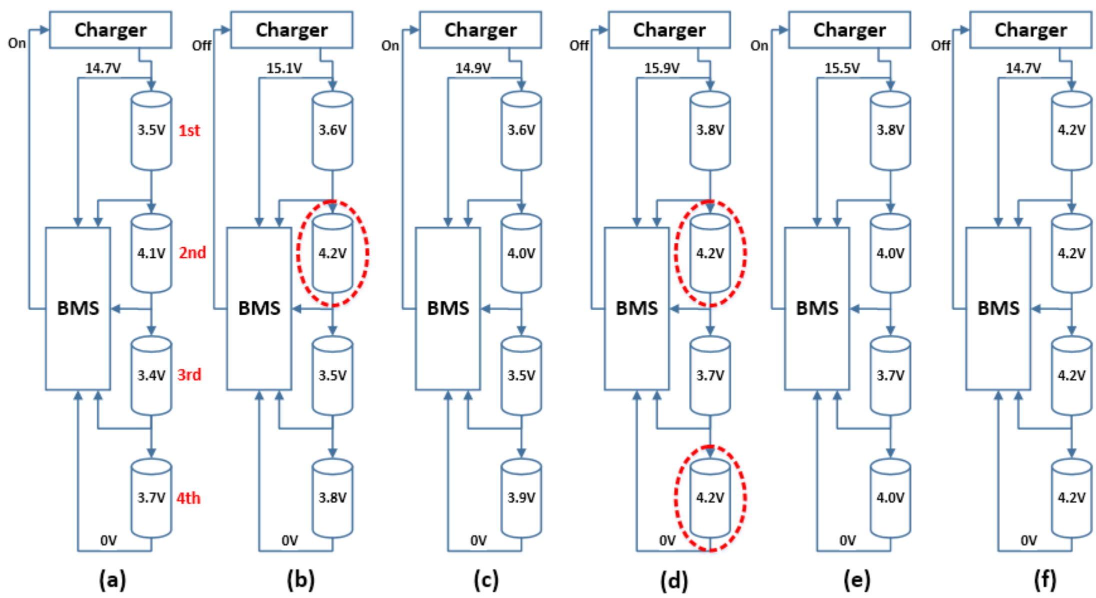

Figure 5.1 : Illustration of balancing during charging [6]

5.1.1 Constant current constant voltage charging

For charging the battery pack, a constant current-constant voltage (CCCV) charger model is used. CCCV chargers are standard regulated power supplies that are used to charge batteries. They are limited in two ways. Initially, the battery is charged at constant current. When the battery is nearly full, its voltage reaches the constant voltage setting of the charger, and the current decays exponentially as the battery gets a finishing charge.

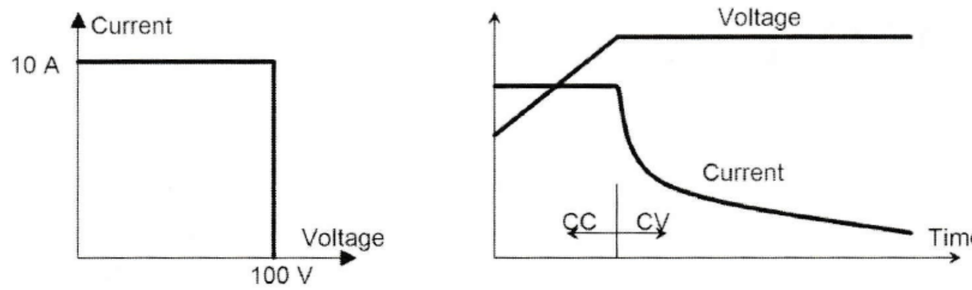

Figure 5.2 : Charging is limited in both current and voltage level, if voltage level is reached, current will be chopped-off.

5.1.2 Simulink implementation

A simulation model is developed to simulate the balancing mechanism, considering 16 Li-ion cells, and voltage and current sensors for each cell. In order to create the balancing mechanism, a bleeding resistor, a diode, and a logical gate (MOSFET) is added for each cell, the structure can be seen in figure 5.3.

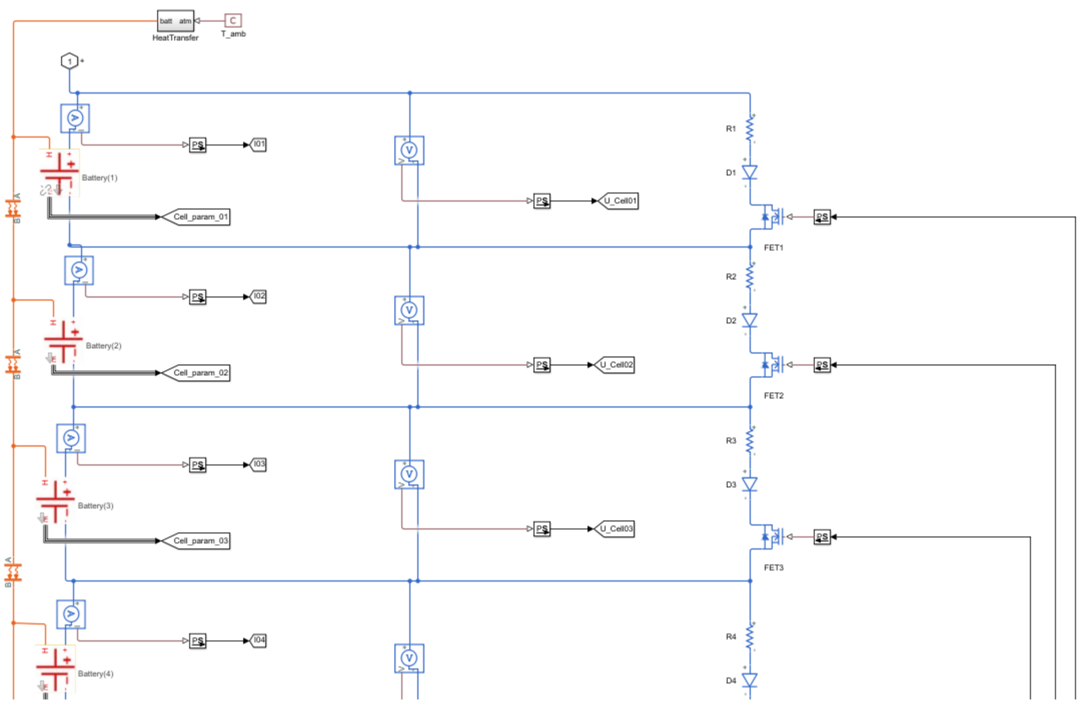

Figure 5.3 : Balancing mechanism in the battery pack.

Next, bleeding resistors are connected in parallel with the output of each Li-ion cells to discharge the excessive charge from the cells with higher SOC. The switches of the bleeding resistors are turned on and off by the balancing logic. A passive balance algorithm is implemented and used for controlling the logical gates of the bleeding resistors. By this way, we eliminated the possibility of premature stopping of charging resulted from an overcharged cell in the battery pack.

5.1.2.1 Simulation results

To this aim, the cells are initialized at random SOC's, and the balancing mechanism is tested during resting, charging, and discharging. In the figure below, it can be seen that all of the cell SOC's are started at different points, and the minimum SOC, which was 50% for this case, is successfully identified by the balancing algorithm.

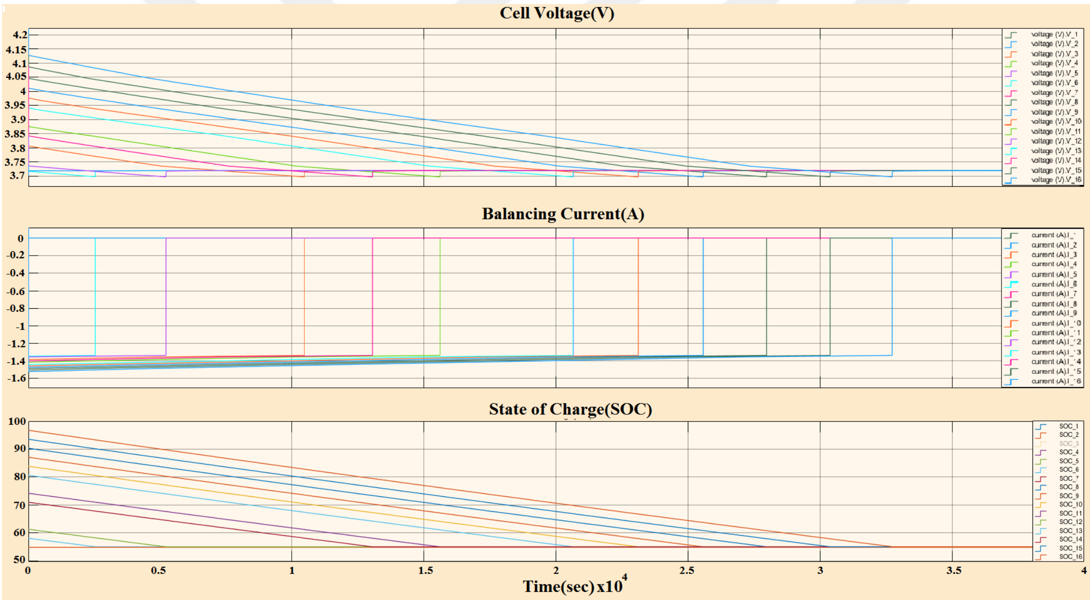

Figure 5.4 : Balancing results in the battery pack.

As can be seen in Figure 5.4, balancing currents are drawn from each cell in a controlled manner via the MOSFET's, until all of the SOC's become equal.

6. CONCLUSION AND RECOMMENDATIONS

This thesis presents an equivalent circuit model able to simulate the dynamic behavior of the studied 51Ah lithium-ion NMC battery cell for EV applications. The main contribution of the study resides in the model calibration and validation, based on the laboratory data recorded during the chassis dynamometer test operations carried out on an HEV currently on the development phase for mass production.

The dynamometer measurement data from two duty cycles tests have been used to this purpose (i.e., HPPC and WLTP). From the data collected on the HPPC, the calibration parameters of the model (i.e., OCV, capacity, and the RC-parameters) have been procured. The parameter tuning process allows configuring the battery model parameters employing an optimization algorithm using HPPC battery load profiles at different temperatures. Then, the obtained parameters at each temperature are merged separately, resulting in the model parameters to depend on SOC and temperature. Later, the model has been validated employing the WLTP duty cycle, pointing that the model is able to reproduce battery transients during operation within 1% accuracy. The primary advantage of this equivalent circuit model is that the momentary behavior of various battery chemistries can be adopted by using the same model but only modifying the model parameters.

6.1 Recommendations and Future Work

In the presented work SOC and temperature dependence of model parameters are covered, but it is important to note that aging effects on RC parameters are not considered. Although the battery model was able to simulate terminal voltage within 1% accuracy under different load conditions, this accuracy will be prone to decrease over time because of cell aging. For future work, working on aging and its effects on a battery cell is strongly recommended to keep simulations precise during the lifetime of the battery.

The temperature kept as an input to the model, but it is also possible to simulate thermal behavior on a pack level. Hence, another essential upgrade to the model would be adding thermal simulations to the model.

REFERENCES

[1] **Park, J.** (2012). *Principles and Applications of Lithium Secondary Batteries*, EngineeringPro collection, Wiley, https://books.google.com.tr/books?id=papHH-urMVYC.

[2] **Linse, C. and Kuhn, R.** (2015). *Design of high-voltage battery packs for electric vehicles*, Elsevier Ltd., http://dx.doi.org/10.1016/B978-1-78242-377-5.00010-8.

[3] **Ciortea, F.**, **Rusu, C.**, **Nemes, M. and Gatea, C.** (2017). Extended kalman filter for state-of-charge estimation in electric vehicles battery packs, *Proceedings - 2017 International Conference on Optimization of Electrical and Electronic Equipment, OPTIM 2017 and 2017 Intl Aegean Conference on Electrical Machines and Power Electronics, ACEMP 2017*, 611–616.

[4] **Bmw**, (2018), WLTP or Worldwide Harmonized Light Vehicles Test Procedure, https://www.bmw.com/en/innovation/wltp.html.

[5] **Shen, Y.** (2018). Adaptive extended Kalman filter based state of charge determination for lithium-ion batteries, *Electrochimica Acta*, *283*, 1432–1440, https://doi.org/10.1016/j.electacta.2018.07.078.

[6] **Andrea, D.** (2010). *Battery Management Systems for Large Lithium Ion Battery Packs*, EBL-Schweitzer, Artech House, https://books.google.com.tr/books?id=o-QpFOR0PTcC.

[7] **Schott, B.**, **Püttner, A. and Müller, M.**, (2015). 3 - The market for battery electric vehicles, **B. Scrosati**, **J. Garche and W. Tillmetz**, editors, Advances in Battery Technologies for Electric Vehicles, Woodhead Publishing Series in Energy, Woodhead Publishing, pp.35 – 54, http://www.sciencedirect.com/science/article/pii/B9781782423775000030.

[8] **Farag, M.S.** (2013). Lithium-Ion Batteries: Modelling and State of Charge Estimation, 169.

[9] **Yang, D.**, **Wang, Y.**, **Pan, R.**, **Chen, R. and Chen, Z.** (2018). State-of-health estimation for the lithium-ion battery based on support vector regression, *Applied Energy*, *227*(March), 273–283, http://dx.doi.org/10.1016/j.apenergy.2017.08.096.

[10] **Zhang, X.**, **Wang, Y.**, **Liu, C. and Chen, Z.** (2018). A novel approach of battery pack state of health estimation using artificial intelligence optimization

algorithm, *Journal of Power Sources*, *376*(September 2017), 191–199, https://doi.org/10.1016/j.jpowsour.2017.11.068.

[11] **Lin, C.**, **Xing, J. and Tang, A.** (2017). Lithium-ion Battery State of Charge/State of Health Estimation Using SMO for EVs, *Energy Procedia*, *105*, 4383–4388, http://dx.doi.org/10.1016/j.egypro.2017.03.931.

[12] **Zhou, X.**, **Stein, J.L. and Ersal, T.** (2017). Battery state of health monitoring by estimation of the number of cyclable Li-ions, *Control Engineering Practice*, *66*(April), 51–63, http://dx.doi.org/10.1016/j.conengprac.2017.05.009.

[13] **Süd, T.** Meeting International Automotive Emissions and Fuel Efficiency Regulations Revisions in emissions requirements and testing procedures will introduce compliance challenges for automotive manufacturers, http://www.tuv-sud.com/uploads/images/1492073398056822630912/tuv-sud-automotive-whitepaper-lr.pdf.

[14] **Simic, D.**, **Dvorak, D.**, **Lacher, H.**, **Kuehnelt, H.**, **Paffumi, E. and De Gennaro, M.** (2014). Modeling and Validation of Lithium-Ion Battery based on Electric Vehicle Measurement, *SAE 2014 World Congress and Exhibition*, SAE International, https://0-doi-org.divit.library.itu.edu.tr/10.4271/2014-01-1850.

[15] **Pavlovic, J.**, **Tansini, A.**, **Fontaras, G.**, **Ciuffo, B.**, **Garcia Otura, M.**, **Trentadue, G.**, **Suarez Bertoa, R. and Millo, F.** (2017). The Impact of WLTP on the official fuel consumption and electric range of Plug - in Hybrid Electric Vehicles in Europe Author , co-author (Do NOT enter this information . It will be pulled from participant tab in, *SAE International*, 1–10, http://papers.sae.org/2017-24-0133/.

[16] **Yao, L.W.**, **Prayun, W.A.**, **Abdul Aziz, M.J.B. and Sutikno, T.** (2015). Battery State-of-Charge Estimation with Extended Kalman-Filter using Third-Order Thevenin Model, *TELKOMNIKA (Telecommunication Computing Electronics and Control)*, *13*(2), 401.

[17] **Huria, T.**, **Ceraolo, M.**, **Gazzarri, J. and Jackey, R.** (2013). Simplified Extended Kalman Filter Observer for SOC Estimation of Commercial Power-Oriented LFP Lithium Battery Cells, *SAE Technical Paper Series*, *1*.

[18] **Barsukov, Y.** (2005). Battery cell balancing: what to balance and how, *Texas Instruments*, 1–8, http://focus.ti.com/download/trng/docs/seminar/Topic2-BatteryCellBalancing-WhattoBalanceandHow.pdf.

CURRICULUM VITAE

Name Surname: Ozan Özay

Place and Date of Birth: Istanbul - 22.07.1993

E-Mail: ozanozay1@gmail.com

EDUCATION:

- **B.Sc.:** 2016, Istanbul Technical University, Faculty of Electrical and Electronic Engineering, Control and Automation Engineering
- **MIN.:** 2017, Istanbul Technical University, Faculty of Mechanical Engineering, Mechatronics Engineering Minor Program
- **M.Sc.:** 2019, Istanbul Technical University, Graduate School of Science, Engineering and Technology, Mechatronics Engineering

PROFESSIONAL EXPERIENCE:

- FEV Türkiye - Electric Vehicle System Engineer (2018 - ...)